Article

ALDH4A1 is an atherosclerosis auto-antigen targeted by protective antibodies

Check for updates

Cristina Lorenzo[1], Pilar Delgado[1,6], Christian E. Busse[2,7], Alejandro Sanz-Bravo[1,7], Inmaculada Martos-Folgado[1,7], Elena Bonzon-Kulichenko[3,4,7], Alessia Ferrarini[3], Ileana B. Gonzalez-Valdes[3], Sonia M. Mur[1], Raquel Roldán-Montero[5], Diego Martinez-Lopez[5], Jose L. Martin-Ventura[4,5], Jesús Vázquez[3,4], Hedda Wardemann[2] & Almudena R. Ramiro[1✉]

Cardiovascular disease (CVD) is the leading cause of mortality in the world, with most CVD-related deaths resulting from myocardial infarction or stroke. The main underlying cause of thrombosis and cardiovascular events is atherosclerosis, an inflammatory disease that can remain asymptomatic for long periods. There is an urgent need for therapeutic and diagnostic options in this area. Atherosclerotic plaques contain autoantibodies[1,2], and there is a connection between atherosclerosis and autoimmunity[3]. However, the immunogenic trigger and the effects of the autoantibody response during atherosclerosis are not well understood[3–5]. Here we performed high-throughput single-cell analysis of the atherosclerosis-associated antibody repertoire. Antibody gene sequencing of more than 1,700 B cells from atherogenic $Ldlr^{-/-}$ and control mice identified 56 antibodies expressed by in-vivo-expanded clones of B lymphocytes in the context of atherosclerosis. One-third of the expanded antibodies were reactive against atherosclerotic plaques, indicating that various antigens in the lesion can trigger antibody responses. Deep proteomics analysis identified ALDH4A1, a mitochondrial dehydrogenase involved in proline metabolism, as a target antigen of one of these autoantibodies, A12. ALDH4A1 distribution is altered during atherosclerosis, and circulating ALDH4A1 is increased in mice and humans with atherosclerosis, supporting the potential use of ALDH4A1 as a disease biomarker. Infusion of A12 antibodies into $Ldlr^{-/-}$ mice delayed plaque formation and reduced circulating free cholesterol and LDL, suggesting that anti-ALDH4A1 antibodies can protect against atherosclerosis progression and might have therapeutic potential in CVD.

Atherosclerosis is a chronic inflammatory disease that leads to the formation of atheroma plaques in the arteries and is the main underlying cause of thrombosis, ischaemic heart disease and stroke[6]. The inflammatory reaction during atherosclerosis is believed to be triggered by the retention and subsequent oxidation (ox) of low-density lipoprotein (LDL) in the vessel sub-endothelium space[7]. In addition, the adaptive arm of the immune response is known to be critical during atherosclerosis[8–10]. Antibodies were first detected in atheroma plaques decades ago, and both protective and pathogenic functions have been attributed to B cells and the antibody immune response during atherosclerosis development[3,11–16]. However, knowledge about the underlying antigenic triggers of this response and their effects on atherosclerosis[3] remains limited, as most studies have focused on oxidation-specific neoepitopes (OSEs) such as those contained in oxLDL[17–22]. Here, we performed an unbiased, high-throughput single-cell study of the antibody repertoire associated with atherosclerosis and identified an antibody–antigen pair with strong diagnostic and therapeutic potential.

To study the antibody immune response associated with atherosclerosis, we made use of $Ldlr^{-/-}$ mice, which develop atherosclerosis when fed a high-cholesterol and fat-diet (HFD). We were interested in assessing germinal centre responses, in which B cells undergo secondary antibody diversification by class switch recombination (CSR) and somatic hypermutation (SHM) and develop into memory B cells and high affinity plasma cells[23]. HFD-fed $Ldlr^{-/-}$ mice ($Ldlr^{-/-}$ HFD mice) progressively accumulated germinal centre B cells (Fas^{+}GL7^{+}), T follicular helper cells (T$_{FH}$; CXCR5^{+}PD1^{+}), memory B cells (PD-L2^{+}), IgG^{+} switched B cells and CD138^{+}kappa^{+} (expressing the kappa light chain) plasma cells or plasmablasts (Fig. 1a, Extended Data Figs. 1, 2a–c, 3a, b). This response was accompanied by increased plasma IgM and IgG and accumulation of IgM antibodies against LDL, malondialdehyde-modified (MDA)-LDL and HSP60 (Extended Data Fig. 2d, e), as found in other atherosclerotic backgrounds[24,25]. To analyse the germinal centre response in atherosclerosis, we performed high-throughput single-cell antibody

[1]B Lymphocyte Biology Lab, Centro Nacional de Investigaciones Cardiovasculares (CNIC), Madrid, Spain. [2]Division of B Cell Immunology, German Cancer Research Center, Heidelberg, Germany. [3]Cardiovascular Proteomics Lab, Centro Nacional de Investigaciones Cardiovasculares (CNIC), Madrid, Spain. [4]CIBER de Enfermedades Cardiovasculares (CIBERCV), Madrid, Spain. [5]Vascular Pathology Lab, IIS-Fundación Jiménez Díaz-Universidad Autónoma, Madrid, Spain. [6]Present address: Centro de Biología Molecular Severo Ochoa, Consejo Superior de Investigaciones Científicas, Universidad Autónoma de Madrid, Madrid, Spain. [7]These authors contributed equally: Christian E. Busse, Alejandro Sanz-Bravo, Inmaculada Martos-Folgado, Elena Bonzon-Kulichenko. ✉e-mail: aramiro@cnic.es
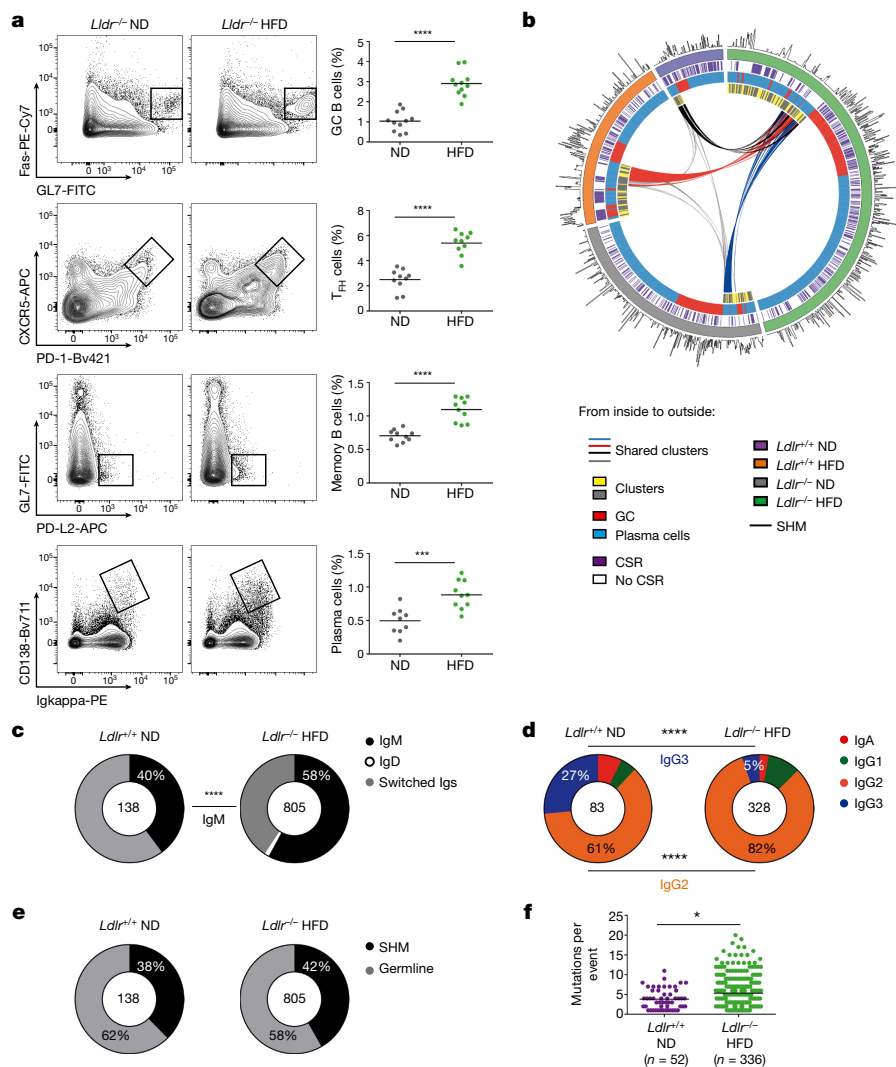
Fig. 1 | The antibody immune response during atherosclerosis. a, $Ldlr^{-/-}$ pro-atherogenic mice were fed either a normal diet (ND) or a high-fat diet for 16 weeks. Representative flow cytometry plots and corresponding quantified data are shown for spleen germinal centre (GC) B cells (Fas$^+$GL7$^+$, gated on B220$^+$; n = 11 mice), T_{FH} cells (CXCR5$^+$PD-1$^+$, gated on CD4$^+$; n = 10 mice), memory B cells (PD-L2$^+$, gated on B220$^+$; n = 10 mice), and plasma cells (CD138$^+$Igκ$^+$; n = 9 $Ldlr^{-/-}$ ND and 10 $Ldlr^{-/-}$ HFD mice). ****P < 0.0001, ***P = 0.0006; two-tailed unpaired Student's t-test. **b**, Circos plot of the molecular features of the 1,727 antibodies sequenced from $Ldlr^{+/+}$ ND mice (n = 138 antibodies), $Ldlr^{+/+}$ HFD

mice (n = 347 antibodies), $Ldlr^{-/-}$ ND mice (n = 437 antibodies), and $Ldlr^{-/-}$ HFD mice (n = 805 antibodies). The plot indicates cell of origin (germinal centre or plasma cells), CSR and SHM, and antibody clusters. **c**, Proportion of IgM, IgD and class-switched immunoglobulins in each group. P < 0.0001; two-sided Fisher exact test. **d**, IgA, IgG1, IgG2 and IgG3 isotype subclass distribution within class-switched events. ****P < 0.0001; two-sided Fisher's exact test. **e**, Proportion of mutated (SHM) and germline antibodies in each group. **f**, Number of somatic IgH mutations within mutated antibodies. *P = 0.0119; two-sided Mann–Whitney test.

repertoire gene sequencing[26] of germinal centre B cells and plasma cells from $Ldlr^{-/-}$ HFD and control mice (Extended Data Fig. 3c). Paired sequences for immunoglobulin heavy (IgH) and light (IgL) chain genes were obtained from more than 1,700 B cells (Fig. 1b, Extended Data Fig. 3d, e). We found no differences in variable (V) and joining (J) gene usage or in CDR3 length between $Ldlr^{-/-}$ HFD and control mice (Extended Data Fig. 3f–h). However, $Ldlr^{-/-}$ HFD mice showed a skewed isotype distribution of class-switched antibodies, with a higher proportion of IgG2 subtypes and a lower proportion of IgG3 subtypes (Fig. 1c, d) and a higher SHM load (Fig. 1e, f). Atherosclerosis is thus associated with enhanced germinal centre B cell responses characterized by increased SHM load and IgG2 bias.

To determine whether the atherosclerosis-associated response was directed against known target antigens, we first identified clusters of

antibodies produced by in-vivo-expanded B cells based on identical V(D)J usage of IgH and IgL and identical IgH CDR3 length (Extended Data Fig. 4a, Supplementary Table 1). We selected 56 such antibodies representing 30 clusters from $Ldlr^{-/-}$ HFD mice for expression (Extended Data Fig. 3c, 4b). As controls, we cloned and expressed 25 antibodies from B cells from wild-type mice fed a normal diet ($Ldlr^{+/+}$ ND mice) (Extended Data Fig. 3c, Supplementary Table 2). $Ldlr^{-/-}$ HFD mice had a slightly, but not significantly, higher fraction of antibodies against MDA-LDL, native LDL and HSP60 (Extended Data Fig. 4c, Supplementary Tables 3, 4). We did not detect polyreactivity in antibodies from either group of mice (Extended Data Fig. 4d). To determine whether the atherosclerosis-associated antibodies recognized plaque lesions, we performed immunofluorescence staining of aortic sinus sections from atherosclerotic mice. One-third (18/56) of the antibodies cloned from $Ldlr^{-/-}$ HFD mice were reactive
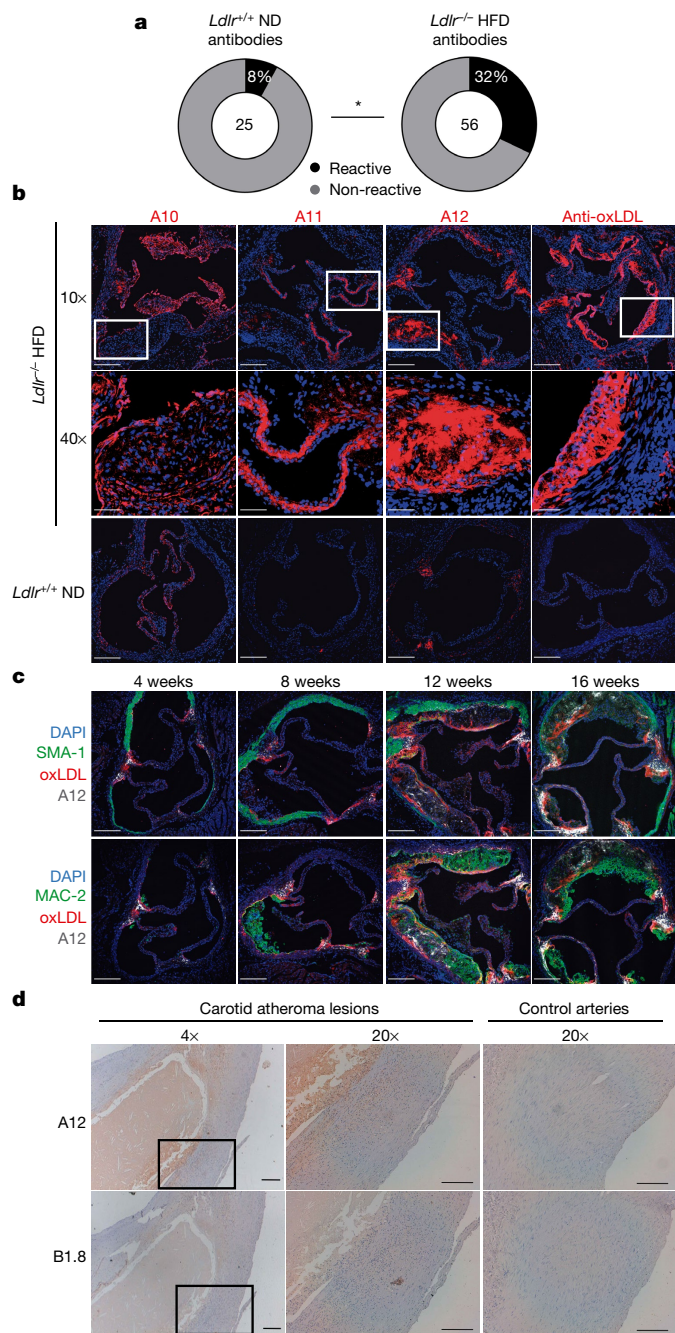
Fig. 2 | Antibodies cloned from atherosclerotic mice show plaque reactivity. a–c, Atheroma plaque reactivity was tested by immunofluorescence in aortic sinus cryosections from *Ldlr*⁻/⁻ HFD mice. The human version of the antibodies (huIgG1) was used for immunofluorescence in mouse tissue. **a**, Proportion of antibodies showing atheroma plaque reactivity (2/25 *Ldlr*⁺/⁺ ND and 18/56 *Ldlr*⁻/⁻ HFD). *P* = 0.0251; two-sided Fisher's exact test. **b**, Immunofluorescence staining with the plaque-reactive antibodies A10, A11 and A12 (cloned from *Ldlr*⁻/⁻ HFD mice) in aortic sinus cryosections from *Ldlr*⁻/⁻ HFD mice and wild-type mice. Right, staining with an anti-oxLDL antibody. **c**, Effects of HFD duration (shown at top) on immunofluorescence staining of aortic sinus from *Ldlr*⁻/⁻ HFD mice with A12 (white), anti-oxLDL (red), and either anti-SMA-1 (top, green) or anti-MAC-2 antibodies (bottom, green). Nuclei were stained with DAPI (blue). **b, c**, Scale bars: 10×, 200 μm; 40×, 50 μm. Maximum intensity *Z*-projection images are shown. **d**, Immunohistochemical staining with A12 or B1-8 anti-NP antibody on paraffin-embedded sections of human carotid atherosclerotic lesions and control arteries. The mouse version of the antibodies (mIgG2b) was used for immunohistochemistry in human tissue. Scale bars, 100 μm.

against atherosclerotic plaques, compared with only 8% (2/25) of the antibodies from *Ldlr*⁺/⁺ ND mice (Fig. 2a, Extended Data Fig. 5, Supplementary Tables 3, 4). The self-reactive antibodies showed diverse patterns of plaque reactivity that were also distinct from the staining pattern observed with a commercial anti-oxLDL antibody (Fig. 2b, Extended Data Fig. 5). These results indicate that the humoral immune response during atherosclerosis targets a variety of antigens in the atherosclerotic plaque.

To investigate the specificity of the atherosclerosis-associated antibody response, we focused on antibody A12, which showed strong plaque reactivity in the aortic sinus in *Ldlr*⁻/⁻ HFD mice. Plaque reactivity of A12 increased during disease progression (Fig. 2b, c) and was mostly extracellular (Fig. 2c, Extended Data Fig. 6a). Notably, A8, a clonally related antibody, also showed strong plaque reactivity. We found that A12 also stained the aortic root of *Ldlr*⁻/⁻ HFD mice (Extended Data Fig. 6b), and aortas from ApoE-deficient mice (an alternative mouse model of atherosclerosis) (Extended Data Fig. 6c). In addition, we detected A12 staining within spleen follicles of *Ldlr*⁻/⁻ HFD mice (Extended Data Fig. 6d). Consistent with A12 being cloned from a splenic B cell, this finding suggests that the A12 target antigen(s) can circulate to or be expressed in the spleen, where they could be involved in triggering a response. Staining of liver sections revealed enhanced and altered A12 reactivity around hepatic veins in *Ldlr*⁻/⁻ HFD atherosclerotic mice, indicating that shifts in distribution or expression of A12 antigen(s) are not limited to arteries (Extended Data Fig. 6e). Notably, A12 also showed reactivity with human atherosclerotic lesions (Fig. 2d). A12 thus recognizes an antigen that is abnormally expressed during atherosclerosis in mouse models and humans.

To determine the antigen specificity of A12, we immunoprecipitated total aorta extracts from *Ldlr*⁻/⁻ HFD or *Ldlr*⁺/⁺ ND mice with A12, and then carried out high-throughput mass spectrometry (Fig. 3a). As controls for specificity, we analysed immunoprecipitates with other antibodies cloned from atherogenic and control mice (A10, A11, D7CT, E9CT), as well as the B1-8 antibody, which is not related to atherosclerosis. A12, but none of the control antibodies, precipitated aldehyde dehydrogenase 4 family member A1 (ALDH4A1), a mitochondrial matrix dehydrogenase of the proline degradation pathway[27] (Fig. 3b, Extended Data Fig. 7a). A12 also precipitated ALDH4A1 from control wild-type aortas (Fig. 3b, Extended Data Fig. 7a), suggesting that A12 does not recognize an atherosclerosis-specific neoepitope. The specificity of A12 for ALDH4A1 was confirmed by enzyme-linked immunosorbent assay (ELISA), by immunoprecipitation followed by blotting with a commercial anti-ALDH4A1 antibody, and by competition ELISA (Fig. 3c, Extended Data Fig. 7b, c). Staining of aortic sinus sections with a commercial anti-ALDH4A1 antibody revealed plaque reactivity similar to that of A12 (Extended Data Fig. 7f). Furthermore, anti-ALDH4A1 antibody showed the same reactivity pattern as A12 around hepatic veins in *Ldlr*⁻/⁻ HFD atherosclerotic mice (Extended Data Figs. 6e, 7g). Notably, anti-ALDH4A1 antibodies were measured at high titres in the plasma of *Ldlr*⁻/⁻ HFD and *Apoe*⁻/⁻ HFD mice but not in controls, and they accumulated during the progression of atherosclerosis (Fig. 3d, Extended Data Fig. 7d, e). Moreover, immunization of wild-type or *Ldlr*⁻/⁻ mice with ALDH4A1 triggered a T cell-dependent immune response and the accumulation of anti-ALDH4A1 IgG1 antibodies (Extended Data Fig. 8). Together, these results identify ALDH4A1 as the target antigen for A12 and show that ALDH4A1 can elicit a T cell-dependent antigen-specific immune response, which associates with high anti-ALDH4A1 IgG plasma titres.

ALDH4A1 was significantly elevated in the plasma of *Ldlr*⁻/⁻ HFD mice (Fig. 3e), and was more abundant in atherosclerotic tissue from humans than in healthy human aortic tissue (Extended Data Fig. 7h). Moreover, analysis of a cohort of patients with carotid
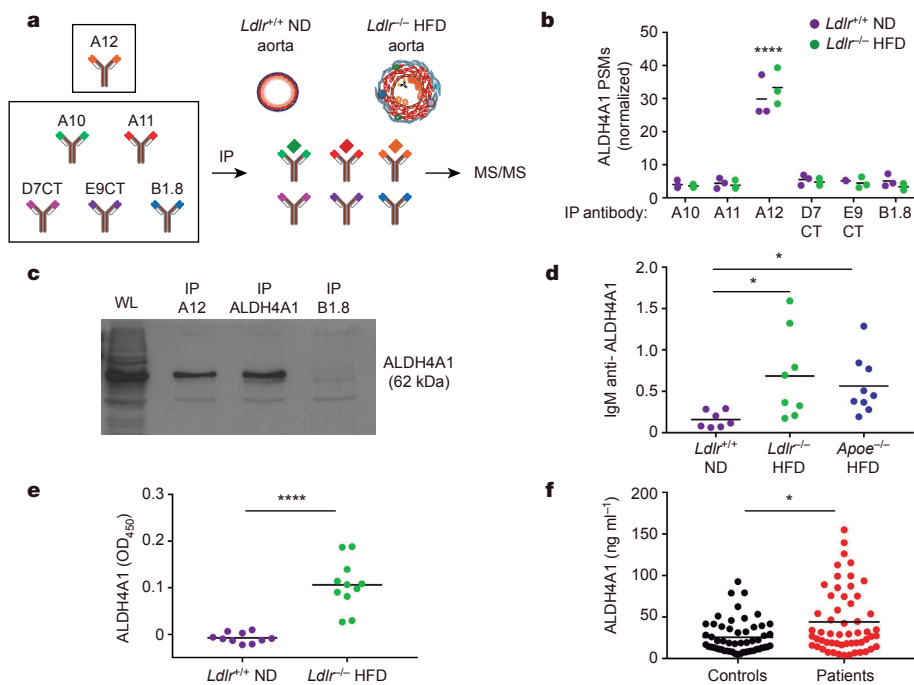
Fig. 3 | ALDH4A1 is a B cell auto-antigen in atherosclerosis. a, Experimental approach used to determine the specificity of antibody A12. Aortic lysates from *Ldlr*^{+/+} ND and *Ldlr*^{−/−} HFD mice were used for immunoprecipitation (IP) with A12 antibody, followed by tandem mass spectrometry (MS/MS) to identify bound proteins. As controls, we used A10 and A11 antibodies from *Ldlr*^{−/−} HFD mice, D7CT and E9CT antibodies from *Ldlr*^{+/+} ND mice, and anti-NP B1-8 antibodies. **b**, Number of normalized peptide spectrum matches (PSMs) identified for ALDH4A1 protein in each immunoprecipitation. ****$P < 0.0001$; two-sided Student *t*-test ($n = 3$ independent experiments). **c**, Validation of specificity of A12 for ALDH4A1 by immunoprecipitation combined with western blot analysis. *Ldlr*^{−/−} HFD total aorta lysate was immunoprecipitated with A12, commercial anti-ALDH4A1 antibody, or anti-NP B1-8 antibody. Precipitates or whole lysate (WL) were then blotted with anti-ALDH4A1 antibody. The expected ALDH4A1 size is indicated (62 kDa). **d**, ELISA determination of anti-ALDH4A1 IgM antibodies in plasma from *Ldlr*^{+/+} ND ($n = 7$), *Ldlr*^{−/−} HFD ($n = 8$), and *Apoe*^{−/−} HFD mice ($n = 9$). *$q = 0.0284$ (*Ldlr*^{−/−} HFD), *$q = 0.0467$ (*Apoe*^{−/−} HFD); one-way ANOVA. **e**, ELISA determination of ALDH4A1 protein in plasma from *Ldlr*^{+/+} ND ($n = 10$) and *Ldlr*^{−/−} HFD mice ($n = 11$). ****$P < 0.0001$; two-tailed unpaired Student *t*-test. OD$_{450}$, optical density at 450 nm. **f**, ELISA determination of ALDH4A1 protein in plasma from human control individuals ($n = 54$) and individuals with carotid atherosclerosis ($n = 56$) *$P = 0.0150$; two-sided Mann–Whitney test.

atherosclerosis revealed significantly elevated plasma ALDH4A1: 23% of patients (13/56) and only 5% of control individuals (3/54) had plasma ALDH4A1 levels of more than 75 ng ml^{-1} (two-tailed Fisher's test, $P = 0.0132$; Fig. 3f). Plasma ALDH4A1 in these patients was associated with the presence of atherosclerosis independently of traditional risk factors and C-reactive protein (CRP) levels (Supplementary Table 5, Extended Data Fig. 7i). Thus, high circulating ALDH4A1 is strongly associated with atherosclerosis, suggesting that ALDH4A1 has potential as biomarker for the disease.

To investigate the effect of A12 antibodies on the progression of atherosclerosis, we performed serial intravenous injections into *Ldlr*^{−/−} HFD mice; for comparison, we injected mice with PBS or a B1-8 IgG2b isotype control antibody (Fig. 4a, Extended Data Fig. 9a, b). After 12 weeks of HFD and regular antibody treatment, mice treated with mA12-IgG2b had smaller plaques than mice treated with the mB1-8-IgG2b control antibody or with PBS alone (Fig. 4b, c). Although we detected no qualitative differences in the cellular or collagen compositions of plaques (Extended Data Fig. 9c–g), mice treated with mA12-IgG2b had lower plasma levels of free cholesterol and LDL (Fig. 4d, e). Notably, quantitative high-throughput proteomic analysis of liver from A12-treated mice identified specific alterations in proteins related to carbohydrate, amino acid and lipid metabolism and immune system and inflammation pathways (Extended Data Fig. 10a–c). Untargeted lipidomics profiling also found alterations in several lipid metabolic pathways, including metabolism of arachidonic acid, a precursor of inflammatory mediators[28,29], and reduction of various triglyceride species (Fig. 4f,

Extended Data Fig. 10d). Hence, both proteomic and metabolomic data indicate that treatment with A12 has a strong effect on lipid and immune pathways in the liver, which can be connected with the systemic lipid alterations observed in A12-treated mice. Together, these results indicate that treatment with the anti-ALDH4A1 A12 antibody reduced the progression of atherosclerosis and improved lipid profiles.

Atherosclerosis is the main underlying cause of thrombosis, and its long asymptomatic phase makes it important to identify individuals at increased risk of cardiovascular events in order to improve the prevention, prediction, diagnosis, and prognosis of CVD[30]. We have adopted an unbiased high-throughput approach to investigate the specificities and functions of novel antibodies in the context of atherosclerosis. Our results show that A12 and its target antigen ALDH4A1 are putative therapeutic and diagnostic tools, respectively, for this disease. Identification of the target antigens of other plaque-reactive antibodies identified in this study will provide further insights in the role of antibodies in atherosclerosis. Although the origin of ALDH4A1 immunogenicity remains unknown, it seems plausible that atherogenic insults that lead to cell death release ALDH4A1 from its secluded mitochondrial niche[31,32]. Such changes in localization or concentration would be likely to trigger an antibody immune response. Further work will be needed to determine whether A12 exerts its protective role in atherosclerosis by clearing ALDH4A1 from damaged tissue. Regardless of the mechanisms involved, our findings identify ALDH4A1 and A12 as promising clinical tools in CVD.
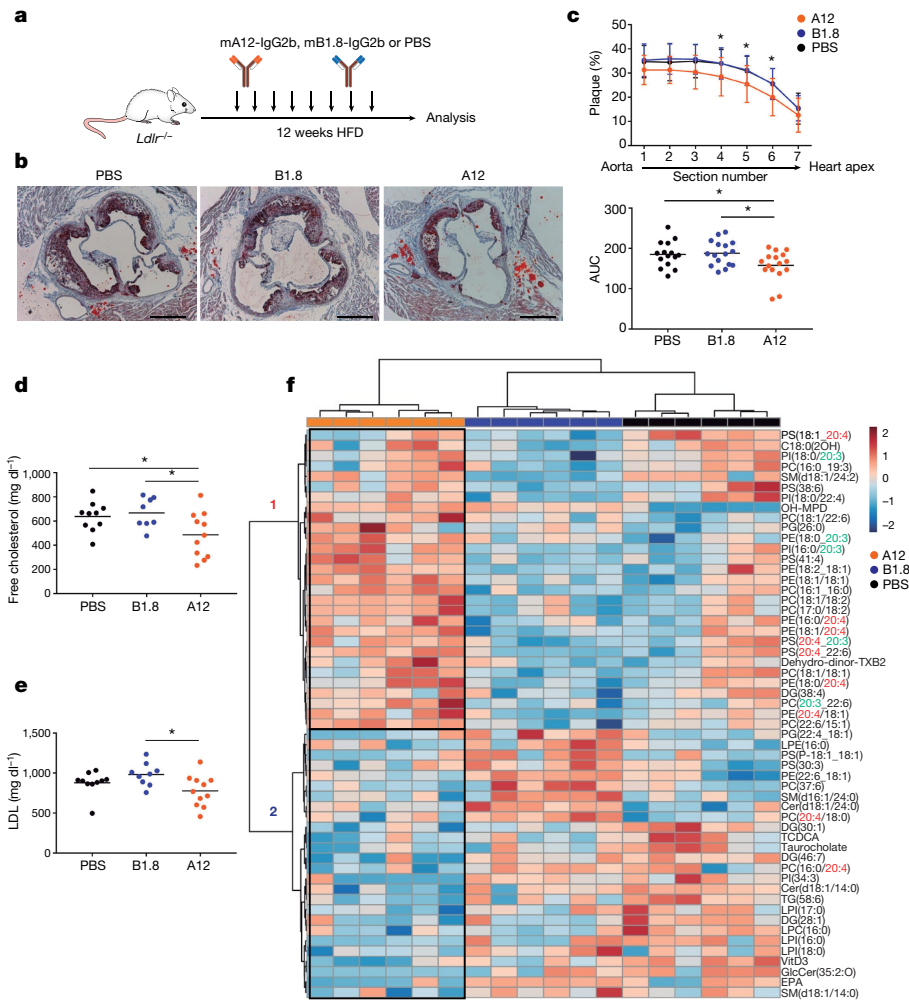
Fig. 4 | A12 infusion delays atherosclerosis progression in *Ldlr*⁻/⁻ HFD mice.
a, Experimental approach. A12 and B1-8 IgH were cloned into an expression vector containing the constant region of mouse IgG2b, the original A12 isotype found in *Ldlr*⁻/⁻ HFD atherosclerotic mice (mA12-IgG2b, mB1-8-IgG2b). *Ldlr*⁻/⁻ mice were injected intravenously with 100 μg mA12-IgG2b (*n* = 16 mice), mB1.8-IgG2b (*n* = 16 mice), or PBS (*n* = 15 mice) every 10 days (arrows) for 12 weeks and fed the HFD throughout. Mouse numbers are summed from two independent experiments. **b**, Representative Oil-Red staining of aortic sinus cryosections from *Ldlr*⁻/⁻ HFD mice treated with PBS, B1.8, or A12. Scale bars, 200 μm. **c**, Top, quantification of atheroma plaque in the mouse aortic sinus (seven sections were quantified per mouse, from the aorta to the heart apex). The proportion of plaque in each section was quantified with Image J. Data are presented as mean ± s.d. *q = 0.0339 (section 4), q = 0.0342 (section 5), q = 0.0331 (section 6); two-way ANOVA. Bottom, area under the curve (AUC) plot of the quantifications above. *q = 0.0430; one-way ANOVA with Benjamini–Hochberg adjustment for multiple comparison. **d**, **e**, Plasma levels of free

cholesterol (top) and LDL (bottom) in *Ldlr*⁻/⁻ HFD mice treated with PBS (*n* = 10 mice), B1.8 (*n* = 8 mice for free cholesterol, *n* = 9 mice for LDL), or A12 (*n* = 11 mice). *q = 0.0462 (free cholesterol), q = 0.0311 (LDL); one-way ANOVA. **f**, Liver lipidomic data for A12-treated mice showing hierarchical clustering analysis. Altered lipids clustered into two populations containing lipids related to glycerophospholipid (GP), sphingolipid, arachidonic acid (AA) and bile acid metabolisms and also with the incorporation into GP of AA (20:4, in red) and its precursor, dihomo-γ-linolenic acid (DGLA; 20:3, in green). C18:0(2OH), dihydroxyoctadecanoate; Cer, ceramide; dehydro-dynor-TXB2, 11-dehydro-2,3-dinor thromboxane B2; DG, diglyceride; EPA, eicosapentaenoic acid; GlcCer, glucocerebroside; LPC, lysophosphatidylcholine; LPE, lysophosphatidylethanolamine; LPI, lysophosphatidylinositol; OH-MPD, hydroxy-methoxy-phenyl-decenone; PC, phosphatidylcholine; PE, phosphatidylethanolamine; PG, phosphatidylglycerol; PI, phosphatidylinositol; PS, phosphatidylserine; SM, sphingomyelin; TCDCA, taurochenodeoxycholic acid; TG, triglyceride; VitD3, diethyl-dihydroxy-dihomo-vitamin D3.

Online content

Any methods, additional references, Nature Research reporting summaries, source data, extended data, supplementary information, acknowledgements, peer review information; details of author contributions and competing interests; and statements of data and code availability are available at https://doi.org/10.1038/s41586-020-2993-2.

1. Hansson, G. K., Bondjers, G., Bylock, A. & Hjalmarsson, L. Ultrastructural studies on the localization of IgG in the aortic endothelium and subendothelial intima of atherosclerotic and nonatherosclerotic rabbits. *Exp. Mol. Pathol.* **33**, 302–315 (1980).
2. Parums, D. & Mitchinson, M. J. Demonstration of immunoglobulin in the neighbourhood of advanced atherosclerotic plaques. *Atherosclerosis* **38**, 211–216 (1981).
3. Sage, A. P., Tsiantoulas, D., Binder, C. J. & Mallat, Z. The role of B cells in atherosclerosis. *Nat. Rev. Cardiol.* **16**, 180–196 (2019).
4. Tsiantoulas, D., Diehl, C. J., Witztum, J. L. & Binder, C. J. B cells and humoral immunity in atherosclerosis. *Circ. Res.* **114**, 1743–1756 (2014).
5. Gisterå, A. & Hansson, G. K. The immunology of atherosclerosis. *Nat. Rev. Nephrol.* **13**, 368–380 (2017).
6. Hansson, G. K. Inflammation, atherosclerosis, and coronary artery disease. *N. Engl. J. Med.* **352**, 1685–1695 (2005).
7. Lusis, A. J. Atherosclerosis. *Nature* **407**, 233–241 (2000).
8. Reardon, C. A. et al. Effect of immune deficiency on lipoproteins and atherosclerosis in male apolipoprotein E-deficient mice. *Arterioscler. Thromb. Vasc. Biol.* **21**, 1011–1016 (2001).
9. Song, L., Leung, C. & Schindler, C. Lymphocytes are important in early atherosclerosis. *J. Clin. Invest.* **108**, 251–259 (2001).
10. Hansson, G. K. & Hermansson, A. The immune system in atherosclerosis. *Nat. Immunol.* **12**, 204–212 (2011).

Article

11. Caligiuri, G., Nicoletti, A., Poirier, B. & Hansson, G. K. Protective immunity against atherosclerosis carried by B cells of hypercholesterolemic mice. *J. Clin. Invest*. **109**, 745–753 (2002).
12. Ait-Oufella, H. et al. B cell depletion reduces the development of atherosclerosis in mice. *J. Exp. Med*. **207**, 1579–1587 (2010).
13. Karvonen, J., Päivänsalo, M., Kesäniemi, Y. A. & Hörkkö, S. Immunoglobulin M type of autoantibodies to oxidized low-density lipoprotein has an inverse relation to carotid artery atherosclerosis. *Circulation* **108**, 2107–2112 (2003).
14. Tsimikas, S. et al. Relationship of IgG and IgM autoantibodies to oxidized low density lipoprotein with coronary artery disease and cardiovascular events. *J. Lipid Res*. **48**, 425–433 (2007).
15. Tay, C. et al. Follicular B cells promote atherosclerosis via T cell-mediated differentiation into plasma cells and secreting pathogenic immunoglobulin G. *Arterioscler. Thromb. Vasc. Biol*. **38**, e71–e84 (2018).
16. Centa, M. et al. Germinal center-derived antibodies promote atherosclerosis plaque size and stability. *Circulation* **139**, 2466–2482 (2019).
17. Palinski, W. et al. Cloning of monoclonal autoantibodies to epitopes of oxidized lipoproteins from apolipoprotein E-deficient mice. Demonstration of epitopes of oxidized low density lipoprotein in human plasma. *J. Clin. Invest*. **98**, 800–814 (1996).
18. Fredrikson, G. N. et al. Identification of immune responses against aldehyde-modified peptide sequences in apoB associated with cardiovascular disease. *Arterioscler. Thromb. Vasc. Biol*. **23**, 872–878 (2003).
19. Chou, M. Y. et al. Oxidation-specific epitopes are dominant targets of innate natural antibodies in mice and humans. *J. Clin. Invest*. **119**, 1335–1349 (2009).
20. Binder, C. J., Papac-Milicevic, N. & Witztum, J. L. Innate sensing of oxidation-specific epitopes in health and disease. *Nat. Rev. Immunol*. **16**, 485–497 (2016).
21. Witztum, J. L. & Lichtman, A. H. The influence of innate and adaptive immune responses on atherosclerosis. *Annu. Rev. Pathol*. **9**, 73–102 (2014).
22. Que, X. et al. Oxidized phospholipids are proinflammatory and proatherogenic in hypercholesterolaemic mice. *Nature* **558**, 301–306 (2018).
23. Victora, G. D. & Nussenzweig, M. C. Germinal centers. *Annu. Rev. Immunol*. **30**, 429–457 (2012).
24. Shaw, P. X. et al. Natural antibodies with the T15 idiotype may act in atherosclerosis, apoptotic clearance, and protective immunity. *J. Clin. Invest*. **105**, 1731–1740 (2000).
25. Tsimikas, S. & Witztum, J. L. Measuring circulating oxidized low-density lipoprotein to evaluate coronary risk. *Circulation* **103**, 1930–1932 (2001).
26. Busse, C. E., Czogiel, I., Braun, P., Arndt, P. F. & Wardemann, H. Single-cell based high-throughput sequencing of full-length immunoglobulin heavy and light chain genes. *Eur. J. Immunol*. **44**, 597–603 (2014).
27. Yoshida, A., Rzhetsky, A., Hsu, L. C. & Chang, C. Human aldehyde dehydrogenase gene family. *Eur. J. Biochem*. **251**, 549–557 (1998).
28. Hanna, V. S. & Hafez, E. A. A. Synopsis of arachidonic acid metabolism: A review. *J. Adv. Res*. **11**, 23–32 (2018).
29. Sonnweber, T., Pizzini, A., Nairz, M., Weiss, G. & Tancevski, I. Arachidonic acid metabolites in cardiovascular and metabolic diseases. *Int. J. Mol. Sci*. **19**, 3285 (2018).
30. Hoefer, I. E. et al. Novel methodologies for biomarker discovery in atherosclerosis. *Eur. Heart J*. **36**, 2635–2642 (2015).
31. Kavurma, M. M., Rayner, K. J. & Karunakaran, D. The walking dead: macrophage inflammation and death in atherosclerosis. *Curr. Opin. Lipidol*. **28**, 91–98 (2017).
32. Bäck, M., Yurdagul, A., Jr, Tabas, I., Öörni, K. & Kovanen, P. T. Inflammation and its resolution in atherosclerosis: mediators and therapeutic opportunities. *Nat. Rev. Cardiol*. **16**, 389–406 (2019).

Methods

Mice

Male low density lipoprotein-receptor deficient ($Ldlr^{-/-}$) mice were obtained from Jackson Laboratories (002207) and fed an HFD containing 22.1% crude fat and 0.2% cholesterol (Ssniff Spezialdiäten) for 4 to 20 weeks when indicated. $Ldlr^{+/+}$ C57BL/6 wild-type mice were obtained from Envigo (C57BL/6JOlaHsd). Apolipoprotein E-deficient ($Apoe^{-/-}$) pro-atherogenic mice were also used (Charles River, B6.129P2-Apoetm1Unc/J), and fed the same HFD described above. All animals were housed in specific pathogen-free conditions, under a 12-h dark–light cycle with food and water ad libitum (room temperature: 20–24 °C; humidity: 45–65%). Sample sizes were chosen to provide confidence in the results and measurements, based on previous studies. The number of mice used in each experiment is indicated in the figure legends and/or Methods. Allocation of mice and samples into groups was random. Data acquisition in all the experiments was performed by experimenters blinded to experimental conditions. Animal procedures were approved by the CNIC Ethics Committee and the Madrid regional authorities (PROEX 377/15) and conformed to EU Directive 2010/63/EU and Recommendation 2007/526/EC regarding the protection of animals used for experimental and other scientific purposes, enforced in Spanish law under Real Decreto 1201/2005.

Human samples

Plasma samples from 56 patients who underwent carotid endarterectomy at IIS-Fundacion Jimenez Diaz and Hospital de Galdako and from 54 control donors with no carotid stenosis were randomly selected (Supplementary Table 5). Control individuals were recruited from a screening program for both carotid atherosclerosis and abdominal aortic aneurysm in 65-year-old men. The absence of vascular disease was confirmed by physical examination and an ultrasound scan. The presence of cardiovascular risk factors such as diabetes mellitus, arterial hypertension, dyslipidaemia and smoking habits were obtained for the logistic regression analysis. Subjects were considered diabetic if they were under treatment (supervised diet, hypoglycaemic oral medication, insulin) or had basal glycaemia >120 mg/dl and/or HbA1c ≥ 6.5%. We defined hypertension as systolic blood pressure (sBP) >140 mm Hg and/or diastolic pressure (dBP) ≥ 90 mm Hg measured during the examination (after the participant had been sitting for at least 30 min) or if the participant was already taking hypotensive medication. Dyslipidaemia was diagnosed as the presence of at least one of the following characteristics: total cholesterol >200 mg/dl, LDL-cholesterol >130 mg/dl, or tryglicerides >200 mg/dl or the participant was already taking statins or fibrates. C-reactive protein (CRP) was measured using an ELISA kit (HycultBiotech). Smoking was defined as 'current smokers' or 'nonsmokers' (including 'ex-smokers', who had stopped smoking at least 6 months before inclusion in the study), with a smoker defined by a history of smoking (≥10 cigarettes per day for >1 year). In some cases, carotid atherosclerotic plaques obtained after endarterectomy were kept in paraformaldehyde for further immunohistological analysis. The Ethical Committee on Human Research at IIS-Fundacion Jimenez Diaz-Autonoma University approved the study, which was performed in accordance with the principles outlined in the Declaration of Helsinki, and all participants gave written informed consent.

Aortic tissue samples were obtained from brain-dead organ donors during removal of organs for therapeutic (kidney or liver) transplantation with the authorization of the French Biomedicine Agency (PFS 09-007, BRIF BB-0033-00029; AoS BBMRI-EU/infrastructure BIOBANQUE; No. Access: 2, Last: April 15, 2014. (BIORESOURCE)). Some of these samples were macroscopically normal and devoid of early atheromatous lesions and were used as healthy controls (H, 9 individuals) for comparison with those with samples with fatty streaks (FS, 7 individuals for media layer and 6 in the case of the intima layer) or fibrolipidic plaques (FL, 11 individuals in the case of media layer and 12 in the case of intima layer)[33].

Flow cytometry

Single-cell suspensions were obtained from spleen and lymph nodes (inguinal and popliteal), blocked with anti-mouse CD16/CD32 antibodies (1/50) and stained with fluorophore or biotin-conjugated anti-mouse antibodies (BD Pharmingen or Biolegend) to detect B220 (RA3-6B2, 1/1,000), Fas (Jo2, 1/100), GL7 (1/200), CD4 (RMY-5, 1/100), CXCR5 (L138D7, 1/100), PD-1 (29F-1A12, 1/100), PD-L2 (TY25, 1/100), CD138 (281-2, 1/100), Igkappa (187.1, 1/500), IgG2b (RMG2b-1, 1/100), IgG2c (polyclonal, 1/100), IgG1 (A85-1, 1/400), IgM (IL-41, 1/100) and IgD (11-26, 1/100). Streptavidin (BD) was used in the case of biotin-conjugated antibodies. Only live lymphocytes were analysed. For Ig-κ intracellular staining, cells were fixated and permeabilized using the Foxp3/Transcription Factor Staining Buffer Set (ThermoFisher Scientific). Samples were acquired on LSRFortessa or FACSCanto instruments (BD Biosciences) using FACSDiva software v6.1.2 and analysed with FlowJo V10.4.2 software.

Immunoglobulin detection in plasma by ELISA

For determination of plasma total IgM and IgG titres, mouse IgM and IgG ELISA Quantitation Kits (Bethyl laboratories) were used according to the manufacturer's instructions. In brief, plates were coated with goat anti-mouse IgM or anti-mouse IgG coating antibodies (1/100), blocked with 1% BSA and incubated with mouse plasmas from different time points (1/25,000 dilution for IgM, 1/50,000 dilution for IgG). For determination of plasma-specific titres for IgM and IgG against prototypic atherosclerosis-associated antigens, plates were coated with MDA-LDL (3 µg/ml, Holzel), native LDL (3 µg/ml, Holzel), Hsp60 (1 µg/ml, Enzo), ALDH4A1-Flag (5 µg/ml) or IKAROS–Flag protein (5 µg/ml) as a control for plasma from immunized mice; blocked with 1% BSA and incubated with mouse plasmas (1/50 dilution for IgM, 1/5 to 1/25 dilution for IgG). Plates were then incubated with goat anti-mouse IgM or anti-mouse IgG detection antibodies conjugated to HRP (1/150,000), followed by TMB substrate solutions. The optical density at 450 nm (OD_{450}) was measured.

Single-cell sorting and sequencing of immunoglobulin transcripts

Single-cell sorting into 384-well plates and Matrix single-cell PCR and sequencing were performed as described[26,34]. In brief, germinal centre B cells (Fas⁺GL7⁺B220⁺) and plasma cells (CD138⁺B220⁻) were isolated from spleen and sorted into lysis buffer-containing wells on an Aria III (BD Biosciences) using single-cell mask settings and FSC-H/FSC-W-based doublet detection. cDNA for the individual cells was generated using random hexamer primers. *Igh*, *Igk* and *Igl* transcripts were amplified using a semi-nested PCR strategy, which in parallel incorporated dual barcodes into the resulting amplicons. To increase the efficiencies for non-class-switched cells, two additional *Ighd* primers were added to the *Igh* PCR master mix in the first and second round of amplification (1° PCR: mIghd-114-rv, 5′-CAGAGGGGAAGACATGTTCAACTAT-3′; 2° PCR: mIghd-079-rv, 5′-CAGTGGCTGACTTCCAATTACTAAAC-3′). Sequencing was performed on 454 GS FLX+ and Illumina MiSeq 2×300, and data were processed using sciReptor[35], versions v1.0.2-3-ga48fc90 and v1.1-2-gf4cf8e2, respectively. Sequence data are available on ENA under study accession number PRJEB34262 and adhere to the MiAIRR data standard[36].

Ig gene cloning and production of recombinant antibodies

Ig gene cloning and production of recombinant antibodies were performed as described previously[37]. In brief, templates from the first scPCR round were amplified with primers containing linker sequences and restrictions sites for cloning. The amplicons were cloned into human IGHG1 (ENA: LT615368; Addgene ID: 80795) and IGKC (ENA:

Article

LT615369; Addgene ID: 80796) expression vectors, respectively, and subsequently Sanger sequenced. The corresponding IgH and IgL chain plasmids were co-transfected into HEK293T cells. Recombinant antibodies were semi-purified from supernatants using Amicon MWCO 30 kDa Ultra Centrifugal Filters (Millipore). IgG concentrations were determined by ELISA.

For functional in vivo experiments, the V regions of the respective Ig heavy and Ig light chain plasmids encoding the A12 and B1-8[38] antibodies were subcloned into mouse *Ighg2b* (ENA: LR588430; Addgene ID: 127155), *Igkc* (ENA: LR588433; Addgene ID: 127157) and *Iglc2* (ENA: LR588434; Addgene ID: 127156) expression vectors, respectively. Expression and purification of recombinant mouse IgG2b antibodies was done as described above. Sequences and cloning strategy were analysed using SeqBuilder software (Lasergene 12.2.0).

Antibody reactivity by ELISA
We coated 96-well plates (Costar) overnight at 4 °C with MDA-LDL (3 μg/ml, Holzel), native LDL (3 μg/ml, Holzel), Hsp60 (1 μg/ml, Enzo) or ALDH4A1–Flag (5 μg/ml) and subsequently blocked them for 1 h with 1% BSA (Sigma). Coated plates were incubated with the recombinant monoclonal antibodies at the indicated concentrations for 1.5 h at room temperature. Bound antibodies were detected with goat anti-human IgG secondary antibody coupled to horse-radish-peroxidase (HRP) (Jackson Immuno Research) diluted 1/1,000 in 1% BSA in PBS, which was then detected using an ABTS substrate solution (Roche). The OD_{405} was determined on a Benchmark Plus microplate spectrophotometer (Bio-Rad). mGO53 antibody was used as a negative control[39].

Polyreactivity ELISA
Polyreactivity ELISAs with positive (ED38 and JB40) and negative (mGO53) control monoclonal antibodies were performed without BSA block after coating with insulin (10 μg/ml, Fitzgerald), double-stranded DNA (10 μg/ml, Sigma) or LPS (10 μg/ml, Sigma L2630) as previously described[39].

Competition ELISA
For competition immunoassays, A12 antibody (1 μg/ml) was preincubated with increasing concentrations (0, 50, 100, 200, or 400 μg/ml) of the indicated competitors (BSA, MDA-LDL or ALDH4A1–Flag) overnight at 4 °C. A12-competitor solutions were added to ELISA plates coated with ALDH4A1–Flag protein (5 μg/ml), and bound A12 antibody was detected as described above. The results are expressed as ratios of A12 binding to ALDH4A1–Flag in the presence (B) or absence (B0) of the competitor.

Immunofluorescence
For tissue immunofluorescence, spleen, heart, aorta and liver specimens were fixed with 4% paraformaldehyde, incubated with 30% sucrose, embedded in OCT compound (Olympus), and frozen in dry ice. Ten-micrometre sections were permeabilized with 0.5% Triton X-100 (Sigma) and blocked with 2% BSA (Sigma) and 5% normal serum (Sigma). The following commercial primary anti-mouse antibodies were used: rat anti-B220 (BD, 1/100), rabbit anti-oxLDL (Acris, 1/400), mouse anti-SMA-1 biotin (ThermoFisher Scientific, 1/200), rat anti-MAC-2 (Tebu-Bio, 1/200) and rabbit anti-fibronectin (Abcam, ab2413); and the following fluorophore-conjugated secondary antibodies (Molecular Probes, 1/500) or streptavidins: goat anti-rat Alexa Fluor 488 or 568, goat anti-rabbit Alexa Fluor 568 and streptavidin Alexa Fluor 488. Germinal centre B cells were stained using lectin PNA Alexa Fluor 647 (Life Technologies). The human version of the antibodies (huIgG1) was used for immunofluorescence in mouse tissue (8–10 μg/ml), in combination with goat anti-human IgG Alexa Fluor 488 or 647 secondary antibodies (Jackson ImmunoResearch, 1/500). Slides were mounted with Prolong Gold (Life Technologies) after DAPI staining and images were taken using a Leica SPE confocal microscope.

Identification of antibody antigens by proteomics analysis
Aortas from *Ldlr*^{−/−} HFD ($n = 27$) and *Ldlr*^{+/+} ND ($n = 30$) mice were homogenized in 1% NP-40, 20 mM Tris-HCl pH 8, 150 mM NaCl and 5% glycerol lysis buffer supplemented with protease and phosphatase inhibitors cocktail (Roche), and the amount of protein was quantified using a Pierce BCA Protein Assay Kit (Thermo Fisher Scientific). Recombinant monoclonal antibodies (A10, A11, A12, D7CT, E9CT and B1-8) were covalently coupled onto an amine-reactive resin using the Pierce Co-Immunoprecipitation Kit (Thermo Fisher Scientific), in accordance with the manufacturer's instructions. Two milligrams of protein extract was pre-cleared by incubating with 50 μl of underivatized agarose beads (co-IP, Pierce) for 30 min at 4 °C. The supernatant was further incubated with 20 μg of resin-coupled antibody overnight at 4 °C. Beads were washed four times with lysis buffer and two times with lysis buffer without detergent. Bound proteins were released from beads by boiling in sample buffer (5% SDS) for 5 min at 95 °C. Immunoprecipitates were resolved by SDS–PAGE and subjected to protein digestion followed by nanoliquid chromatography coupled to MS/MS for protein identification and quantification by spectral counting[40]. Each sample was infused in triplicate. Peptide identification from MS/MS data was performed using the probability ratio method[41]. False discovery rates (FDR) of peptide identifications were calculated using the refined method[42,43]; 1% FDR was used as the criterion for peptide identification.

Quantitative proteomics analysis of human aorta and mouse liver samples
Tissue from human aortas (100 mg of FL, FS or H) was homogenized at low temperature, and resuspended in lysis buffer (50 mM iodoacetamide (Sigma), 1.5% SDS, 1 mM EDTA, 100 mM Tris-HCl, pH 8.5) for protein extraction. Proteins were extracted from mouse liver (50 mg from A12, B1.8 or PBS-treated mice) using 100 mM Tris-HCl pH 7.4, 1 mM EDTA, 4% SDS. The proteins were subjected to filter-aided digestion with trypsin as described[44] using Nanosep Centrifugal Devices with Omega Membrane-10K, PALL, and the resulting peptides were subjected to multiplexed isobaric labelling with TMT reagents (Thermo Fisher Scientific). Each TMT batch contained an internal reference standard containing pooled samples.

Aorta peptides were separated into eight fractions using OASIS MCX cartridges, while the liver peptides were separated into five fractions using the high pH reversed-phase peptide fractionation kit (Thermo Fisher Scientific). Peptide fractions were analysed on an Easy nLC 1000 liquid chromatography system coupled to either a Q-Exactive HF mass spectrometer (Thermo Fisher Scientific) or an Orbitrap Fusion mass spectrometer (Thermo Fisher Scientific). MS/MS data were acquired using Xcalibur (2.2, Thermo Fisher Scientific) and searched on Proteome Discoverer (2.1, Thermo Fisher Scientific). Identification, quantification and statistical and systems biology analysis of coordinated protein behaviour were performed using an in-house developed program (SanXot 1.0) based on published models developed in the J.V. laboratory[41–43,45–47]. Absolute quantitative protein values were calculated by summing up the reporter ion intensities of each of the peptide-spectrum matches corresponding to ALDH4A1, to all mitochondrial proteins or to ACTB, and were expressed as a percentage of the sum of absolute quantitative values of all the proteins identified in the sample. Statistically significant differences between cumulative distributions were assessed using the two-sample Kolmogorov–Smirnov test (*$P < 0.05$, **$P < 0.01$, ***$P < 0.001$, ****$P < 0.0001$). Correlation network analysis was performed in Cytoscape 3.6.1 (https://cytoscape.org/) with the ClusterONE plugin, using Pearson correlation of quantitative values of all possible protein pairs with a correlation coefficient higher than 0.3. ClusterONE settings used were: minimum size 5, minimum density Auto, Edhe weights correlation, Node penalty 2, Merging method single pass, overlap threshold 0.4. Functional enrichment analysis was performed with STRING (11.0)[48]. Proteomics data

are available on Peptide Atlas ftp://PASS01505:VE2555mc@ftp.peptideatlas.org/ and ftp://PASS01607:CP3575gq@ftp.peptideatlas.org/.

Liver lipidomics and metabolomics

Frozen liver tissues were lysed in 0.5× PBS (sample:solvent 1:10 ratio) containing 1 mg/ml butylhydroxytoluene (BHT) solution in methanol (proportion 200 μl/g tissue), with a FastPrep-24 5G instrument (MP Biomedicals, USA). Aliquots of homogenate (25 μl) were collected and stored at −80 °C until lipidomic extraction. Tissue homogenates were thawed and extracted with methyl-tert-butylether (MTBE) as described[49]. Organic phase (900 μl) was dried out in speedvac and resuspended in 50 μl ACN:H_2O (20:80, v-v) just before injection.

Untargeted lipidomics analysis was performed using an Ultimate 3000 HPLC equipped with Agilent mRP-Recovery C18 column (100 × 0.5 mm, 5 μm) thermostated at 55 °C, coupled to an Orbitrap ELITE Hybrid Ion Trap-Orbitrap Mass Spectrometer (ThermoFisher Scientific). Compounds were eluted at 100 μl/min using (A) 5 mM ammonium formate in water in ESI(+) and water with 0.1% formic acid in ESI(−), and (B) 5 mM ammonium formate in 99:1 (v/v) acetonitrile:water in ESI(+) and acetonitrile with 0.1% formic acid in ESI(−). MS was operated in full scan mode from 70 to 1,700 m/z at 60,000 resolution. Data processing was carried-out using the Metaboprofiler node of Compound Discoverer 2.1 (ThermoFisher; USA)[50] and MetaboAnalyst 4.0[51]. Abundance changes in features present in 80% of the samples with a coefficient of variation lower than 30% were analysed by ANOVA. Putative identification of features with a significant change was performed using CEU Mass Mediator 3.0[52] and compounds were identified by the exact mass, isotopic pattern distribution and by the elucidation of MS/MS spectra collected in data-dependent mode at 60,000 resolution, using a top 5 method and dynamic exclusion. Hierachical clustering was performed with MetaboAnalyst 4.0 using the identified features; only the most abundant primary adduct was used in the analysis. Lipid names were according to the Lipid Maps nomenclature[53–55], except for the cases indicated in Fig. 4. Lipidomics data are available at the NMDR website (https://www.metabolomicsworkbench.org/data/DRCCMetadata.php?Mode=Project&ProjectID=PR000985), project ID PR000985.

Validation of proteomics results by Immunoprecipitation and Immunoblotting

Aortas from $Ldlr^{-/-}$ HFD mice (n = 8) were homogenized in 1% NP-40 lysis buffer supplemented with protease and phosphatase inhibitors cocktail (Roche) as in the proteomics experiment. In parallel, recombinant antibodies A12 and B1-8, and an anti-ALDH4A1 antibody (Abcam), were covalently coupled onto an amine-reactive resin using the Pierce Co-Immunoprecipitation Kit (Thermo Fisher Scientific). One milligram of total protein from aorta lysates was used to immunoprecipitate with 10 μg resin-coupled antibody overnight at 4 °C. Elution was done with pH 2.8 elution buffer. Immunoprecipitates were size-fractionated on SDS−PAGE 12% acrylamide-bisacrylamide gels and transferred to Protan nitrocellulose membrane (GE Healthcare). Membrane was probed with rabbit anti-ALDH4A1 (1/10,000, Abcam). Then, the membrane was incubated with anti-rabbit IgG HRP TrueBlot (1/1,000, Rockland) and developed with Amersham ECL Western Blotting Detection Reagent (GE Healthcare Life Sciences). An unprocessed scan of the blot is supplied in Supplementary Fig. 1.

ALDH4A1 recombinant protein production and purification

Mouse ALDH4A1 ORF mammalian expression plasmid, C-Flag tag (Sino Biological) and mouse IKAROS, N-Flag tag (pCMV2) were transfected into HEK293T cells using polyethylenimine (PEI, Sigma). After 72 h, cells were lysed with 50 mM Tris HCl pH 7.4, 150 mM NaCl, 1 mM EDTA and 1% TRITON X-100 lysis buffer supplemented with protease and phosphatase inhibitors cocktail (Roche). ALDH4A1−Flag and IKAROS−Flag proteins were then purified using the anti-Flag M2 Affinity Gel (Sigma), in accordance with the manufacturer's instructions. Elution was performed with the 3× Flag peptide (Sigma), which was then removed using 30-kDa Microcon Centrifugal Filters (Millipore).

ALDH4A1−Flag immunization

C57/BL6 or $Ldlr^{-/-}$ mice (6–7 weeks old) were immunized intraperitoneally with 50 μg ALDH4A1−Flag in PBS and precipitated in alum (Imject Alum, Thermo Scientific) at a 2:1 ratio. After 2 weeks, mice were boosted by subcutaneous injection into the footpads with 50 μg ALDH4A−Flag plus PBS. Seven to eight days after the boost, mice were killed and analysed. Control groups were inoculated twice with PBS or alum and PBS.

Quantification of ALDH4A1 protein levels in plasma by ELISA

Plasma from $Ldlr^{-/-}$ HFD (n = 11) and $Ldlr^{+/+}$ ND mice (n = 10) were used to quantify mouse ALDH4A1 protein levels using the Mouse P5CDH/ALDH4A1 ELISA Kit (LifeSpan BioSciences), in accordance with the manufacturer's instructions. Plasmas were used at 1/4 dilution. In addition, plasma from patients with carotid atherosclerosis (n = 56) and control individuals (n = 54) were used to quantify human ALDH4A1 protein levels using the Human P5CDH/ALDH4A1 ELISA Kit (LifeSpan BioSciences), at 1/10 dilution.

Immunohistochemistry

Mouse hearts and livers were fixed in neutral-buffered 10% formalin solution (Sigma), embedded in paraffin blocks, and cut into 10-μM sections. For immunohistochemistry, sodium citrate buffer was used for antigen retrieval and rabbit anti-ALDH4A1 (1/100, Abcam) antibody was used, followed by a biotinylated goat anti-rabbit antibody (1/200, Abcam). The biotinylated antibody was detected with the ABC system using diaminobenzidine as substrate (Vector Laboratories). Images were acquired with a Leica DM2500 microscope.

Human atherosclerotic plaques were fixed in 3.7% paraformaldehyde, embedded in paraffin and sectioned at 3 μm. Sections were deparaffinized, hydrated and incubated with 6% goat serum, BSA 4% in PBS for 1 h. Sections were incubated with A12, B1-8 or an irrelevant immunoglobulin (Dako) (10 μg/ml, overnight). Sections were then incubated with anti-mouse biotinylated secondary antibody (1/250 dilution, 1 h, Dako) and ABComplex (30 min, Vector lab), followed by staining with 3,30-diaminobenzidine (DAB), haematoxylin counterstaining, and mounting in DPX medium.

Quantification of atherosclerosis development

Ten-week-old male $Ldlr^{-/-}$ mice were treated with a fully mouse version of the A12 antibody (mA12-IgG2b), as originally found in atherosclerotic mice (n = 16). Mice infused with the isotype control antibody mB1.8-IgG2b (n = 16) or with PBS (n = 15) were used as controls. For the infusion, 100 μg of the corresponding antibody in 100 μl PBS was injected intravenously every 10 days over 12 weeks. Mice were fed with HFD for the 12-week duration of the antibody treatment. Saline-perfused hearts were fixed with 4% paraformaldehyde, incubated with 30% sucrose, embedded in OCT compound (Olympus), and frozen in dry ice. Atherosclerotic plaque area was quantified by ImageJ analysis of Oil-Red-O-stained serial 80-μm-spaced cryostat 10-μm cross-sections of aortic sinus, starting from proximal aorta to the heart apex[56]. Atherosclerosis lesions are represented as a percentage of the lesion surface to the total surface of the three valves. The collagen content within atherosclerotic lesions was quantified from Picrosirius Red-stained cross sections. Plasma levels of free cholesterol and LDL were measured using Dimension RxL Max Analyzer (Siemens).

For en face preparations, aortas were fixed with 4% paraformaldehyde for 1 h at room temperature, washed with PBS and stained with Oil-Red-O solution (Merk). Next, they were opened longitudinally using microsurgery scissors (FST) under a Leica lens.

Evaluation of A12 antibody at the atheroma plaque and liver of infused mice

Ten-week-old $Ldlr^{-/-}$ male mice were fed with HFD for 12 weeks, infused intravenously with 100 μg huA12-IgG1 (n = 5), huB1-8-IgG1 (n = 4) or PBS

Article

(n = 4), and killed 3–7 days later. Saline-perfused hearts and livers were fixed with 4% paraformaldehyde, incubated with 30% sucrose, embedded in OCT compound (Olympus), and frozen in dry ice. Ten-micrometre cross sections of aortic sinus and liver were stained with goat anti-human IgG Alexa Fluor 647 antibody (Jackson ImmunoResearch, 1/500) to detect the injected antibody by immunofluorescence.

Statistics and reproducibility

Statistical analysis was performed in GraphPad Prism 7.3. In most cases, the graphs show the mean and, when shown, the error bars represent standard deviation (s.d.). For values that followed a Gaussian distribution (D'Agostino–Pearson omnibus normality test), the two-tailed Student's t-test was used ($P \leq 0.05$ was considered significant; *$P \leq 0.05$, **$P < 0.01$, ***$P < 0.001$, ****$P < 0.0001$) when comparing two groups. One-way or two-way ANOVA tests were used when comparing more than two groups or different time points, respectively ($q \leq 0.05$ was considered significant, after correcting for multiple comparison using the original FDR method of Benjamini and Hochberg; *$q \leq 0.05$, **$q < 0.01$, ***$q < 0.001$, ****$q < 0.0001$). When the values did not follow a Gaussian distribution, the two-tailed Mann–Whitney test was used ($P \leq 0.05$ was considered significant; *$P \leq 0.05$, **$P < 0.01$, ***$P < 0.001$, ****$P < 0.0001$), when comparing two groups. For continuous data, Fisher's exact test for categorical data was used ($P \leq 0.05$ was considered significant; *$P \leq 0.05$, **$P < 0.01$, ***$P < 0.001$, ****$P < 0.0001$). In human patients with carotid atherosclerosis, logistic regression analysis adjusted with cardiovascular risk factors was performed with the presence of atherosclerosis as a dependent variable.

Regarding results from representative experiments, such as micrographs, representative images are shown of: more than three (A10, A11) or more than five (A12) experiments (Fig. 2b); one experiment (Fig. 2c, Extended Data Figs. 7g, 9a, b, f); more than five experiments (Fig. 2d); two experiments (Figs. 3c, 4b, Extended Data Figs. 7f, 9c); three experiments (Extended Data Fig. 3b); one to five experiments (Extended Data Fig. 5); one to three experiments (Extended Data Fig. 6).

Reporting summary

Further information on research design is available in the Nature Research Reporting Summary linked to this paper.

Data availability

Antibody sequences are available from ENA under accession PRJEB34262. Proteomics data are available on Peptide Atlas ftp://PASS01505:VE2555mc@ftp.peptideatlas.org/ and ftp://PASS01607:CP3575gq@ftp.peptideatlas.org/. Lipidomics data are available at the NMDR website (https://www.metabolomicsworkbench.org/data/DRCCMetadata.php?Mode=Project&ProjectID=PR000985), project ID PR000985. Source data are provided with this paper.

33. Martínez-López, D. et al. Complement C5 protein as a marker of subclinical atherosclerosis. *J. Am. Coll. Cardiol.* **75**, 1926–1941 (2020).
34. Murugan, R., Imkeller, K., Busse, C. E. & Wardemann, H. Direct high-throughput amplification and sequencing of immunoglobulin genes from single human B cells. *Eur. J. Immunol.* **45**, 2698–2700 (2015).
35. Imkeller, K., Arndt, P. F., Wardemann, H. & Busse, C. E. sciReptor: analysis of single-cell level immunoglobulin repertoires. *BMC Bioinformatics* **17**, 67 (2016).
36. Rubelt, F. et al. Adaptive Immune Receptor Repertoire Community recommendations for sharing immune-repertoire sequencing data. *Nat. Immunol.* **18**, 1274–1278 (2017).
37. Tiller, T., Busse, C. E. & Wardemann, H. Cloning and expression of murine Ig genes from single B cells. *J. Immunol. Methods* **350**, 183–193 (2009).
38. Bothwell, A. L. et al. Heavy chain variable region contribution to the NP[b] family of antibodies: somatic mutation evident in a γ2a variable region. *Cell* **24**, 625–637 (1981).
39. Wardemann, H. et al. Predominant autoantibody production by early human B cell precursors. *Science* **301**, 1374–1377 (2003).
40. Villarroya-Beltri, C. et al. Sumoylated hnRNPA2B1 controls the sorting of miRNAs into exosomes through binding to specific motifs. *Nat. Commun.* **4**, 2980 (2013).
41. Martínez-Bartolomé, S. et al. Properties of average score distributions of SEQUEST: the probability ratio method. *Mol. Cell. Proteomics* **7**, 1135–1145 (2008).
42. Navarro, P. & Vázquez, J. A refined method to calculate false discovery rates for peptide identification using decoy databases. *J. Proteome Res.* **8**, 1792–1796 (2009).
43. Bonzon-Kulichenko, E., Garcia-Marques, F., Trevisan-Herraz, M. & Vázquez, J. Revisiting peptide identification by high-accuracy mass spectrometry: problems associated with the use of narrow mass precursor windows. *J. Proteome Res.* **14**, 700–710 (2015).
44. Wiśniewski, J. R., Zougman, A., Nagaraj, N. & Mann, M. Universal sample preparation method for proteome analysis. *Nat. Methods* **6**, 359–362 (2009).
45. Navarro, P. et al. General statistical framework for quantitative proteomics by stable isotope labeling. *J. Proteome Res.* **13**, 1234–1247 (2014).
46. García-Marqués, F. et al. A novel systems-biology algorithm for the analysis of coordinated protein responses using quantitative proteomics. *Mol. Cell. Proteomics* **15**, 1740–1760 (2016).
47. Trevisan-Herraz, M. et al. SanXoT: a modular and versatile package for the quantitative analysis of high-throughput proteomics experiments. *Bioinformatics* **35**, 1594–1596 (2019).
48. Szklarczyk, D. et al. STRING v11: protein–protein association networks with increased coverage, supporting functional discovery in genome-wide experimental datasets. *Nucleic Acids Res.* **47**, D607–D613 (2019).
49. Matyash, V., Liebisch, G., Kurzchalia, T. V., Shevchenko, A. & Schwudke, D. Lipid extraction by methyl-tert-butyl ether for high-throughput lipidomics. *J. Lipid Res.* **49**, 1137–1146 (2008).
50. Röst, H. L. et al. OpenMS: a flexible open-source software platform for mass spectrometry data analysis. *Nat. Methods* **13**, 741–748 (2016).
51. Chong, J., Wishart, D. S. & Xia, J. Using MetaboAnalyst 4.0 for comprehensive and integrative metabolomics data analysis. *Curr. Protoc. Bioinformatics* **68**, e86 (2019).
52. Gil-de-la-Fuente, A. et al. CEU Mass Mediator 3.0: a metabolite annotation tool. *J. Proteome Res.* **18**, 797–802 (2019).
53. Fahy, E. et al. Update of the LIPID MAPS comprehensive classification system for lipids. *J. Lipid Res.* **50** (Suppl), S9–S14 (2009).
54. Fahy, E. et al. A comprehensive classification system for lipids. *J. Lipid Res.* **46**, 839–862 (2005).
55. Liebisch, G. et al. Shorthand notation for lipid structures derived from mass spectrometry. *J. Lipid Res.* **54**, 1523–1530 (2013).
56. Venegas-Pino, D. E., Banko, N., Khan, M. I., Shi, Y. & Werstuck, G. H. Quantitative analysis and characterization of atherosclerotic lesions in the murine aortic sinus. *J. Vis. Exp.* **82**, 50933 (2013).

Author contributions A.R.R. conceived the study; C.L., P.D. and A.R.R. designed experiments; C.L., P.D., I.M.-F. and S.M.M. performed FACS experiments; C.L. performed ELISAs, cloning and expression of immunoglobulins, immunofluorescence staining, immunoprecipitation and immunoblotting and functional atherosclerosis experiments; S.M.M. performed immunohistochemistry staining in mouse tissues; A.S.-B. produced ALDH4A1–Flag protein; I.M.-F. and A.S.-B. performed immunization experiments; H.W. conceived B cell analyses; C.E.B. conceived and performed and analysed single-cell sorting and sequencing experiments; I.B.G.-V., E.B.-K., A.F. and J.V. performed and analysed proteomics and metabolomics experiments; R.R.-M., D.M.-L. and J.L.M.-V. performed and analysed the experiments with human samples; C.L. and A.R.R. analysed data and prepared figures; and C.L. and A.R.R. wrote the manuscript. All authors read and approved the final version of the manuscript.

Extended Data Fig. 1 | Flow cytometry analysis of the humoral response associated with atherosclerosis development. a, Representative flow cytometry plots showing the gating strategy used to analyse the humoral response associated to atherosclerosis in the spleen of *Ldlr*$^{-/-}$ mice. **b**, Quantification of the absolute number of germinal centre B cells (Fas$^+$GL7$^+$, gated on B220$^+$) (n = 10 *Ldlr*$^{-/-}$ ND, n = 11 *Ldlr*$^{-/-}$ HFD mice), T follicular helper (Tfh) cells (CXCR5$^+$PD-1$^+$, gated on CD4$^+$) (n = 10 mice), memory B cells (PD-L2$^+$, gated on B220$^+$) (n = 10 mice), plasma cells (CD138$^+$Igκ$^+$) (n = 9 *Ldlr*$^{-/-}$ ND, n = 10 *Ldlr*$^{-/-}$ HFD mice), and class-switched B cells (IgG2b (n = 5 mice), IgG2c (n = 5 mice), IgG1 (n = 7 mice)) in spleens of mice from the indicated groups. Statistical analysis was done with two-tailed unpaired Student's *t*-test.
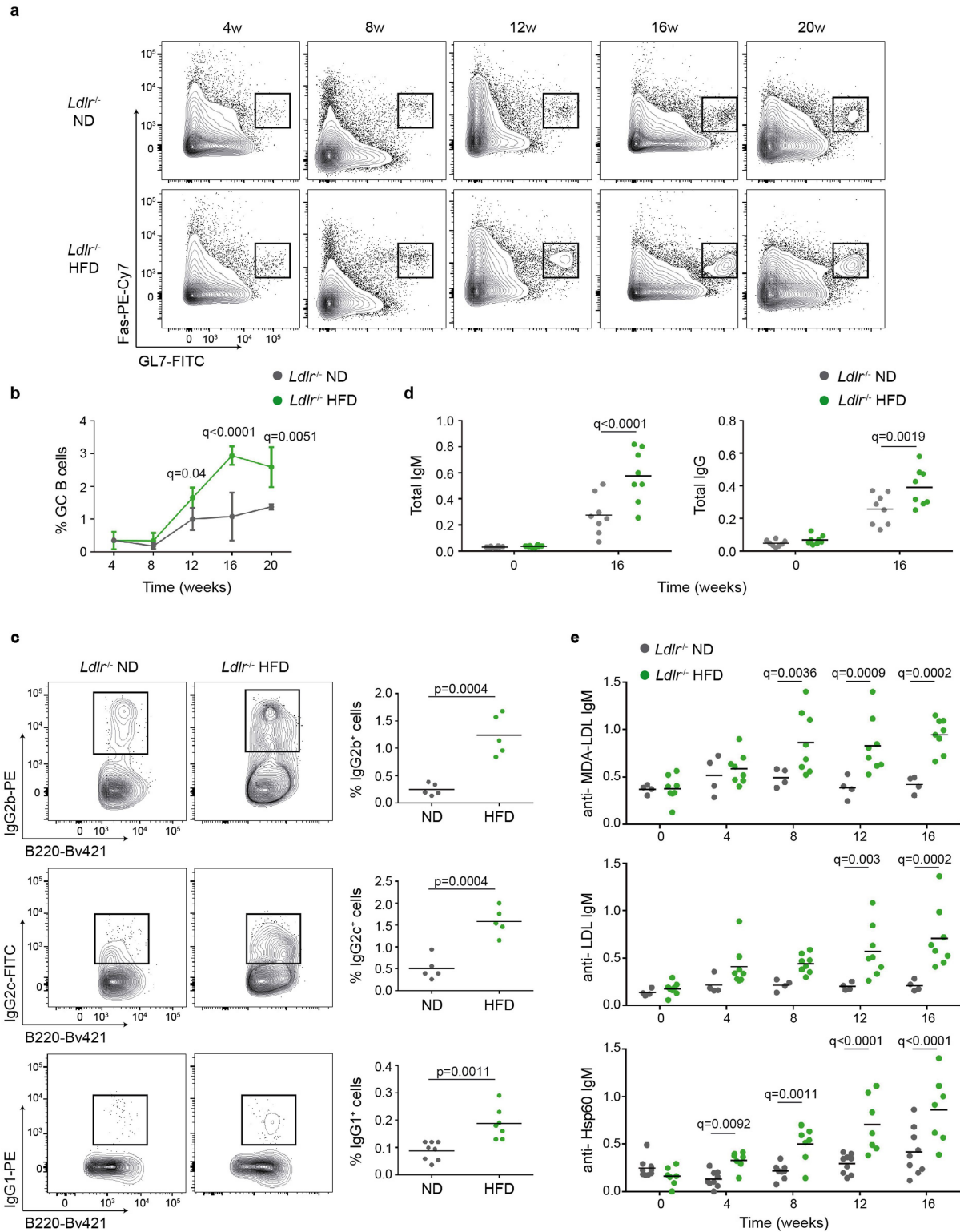
Extended Data Fig. 2 | Germinal centre response and antibody production during atherosclerosis. $Ldlr^{-/-}$ or $Ldlr^{+/+}$ mice were fed either a normal diet (ND) or a high-fat diet (HFD), and the germinal centre response in the spleen was assessed by flow cytometry. **a**, **b**, Analysis of the germinal centre B cells (Fas[+]GL7^{+}, gated on B220[+]) in spleen from $Ldlr^{-/-}$ ND and $Ldlr^{-/-}$ HFD at 4 weeks ($n = 3$ mice), 8 weeks ($n = 3$ mice), 12 weeks ($n = 3$ mice), 16 weeks ($n = 3$ mice) and 20 weeks ($n = 2$ mice) of diet treatment. Representative plots **(a)** and their quantification **(b)** are shown. Data are presented as mean values +/− s.d. Statistical analysis was done with two-way ANOVA. **c**, B cells expressing class-switched immunoglobulins (IgG2b ($n = 5$ mice), IgG2c ($n = 5$ mice), and IgG1 ($n = 8$ $Ldlr^{-/-}$ ND, $n = 7$ $Ldlr^{-/-}$ HFD mice) after 16 weeks of ND/HFD treatment. Statistical analysis was done with two-tailed unpaired Student's t-test. **d**, Plasma from $Ldlr^{-/-}$ mice fed the ND ($n = 8$) or HFD ($n = 8$) was collected at different time points (0 and 16 weeks), and total IgM and IgG levels were determined by ELISA. **e**, Plasma from $Ldlr^{-/-}$ mice fed the ND or HFD was collected at different time points (0, 4, 8, 12, 16 weeks), and IgM antibody titres specific for MDA-LDL ($n = 4$ $Ldlr^{-/-}$ ND, $n = 8$ $Ldlr^{-/-}$ HFD mice), LDL ($n = 4$ $Ldlr^{-/-}$ ND, $n = 8$ $Ldlr^{-/-}$ HFD mice), and Hsp60 ($n = 9$ $Ldlr^{-/-}$ ND, $n = 7$ $Ldlr^{-/-}$ HFD mice) were determined by ELISA. **(d, e)** Data correspond to the relative absorbance at 450 nm. Statistical analysis was done with two-way ANOVA.
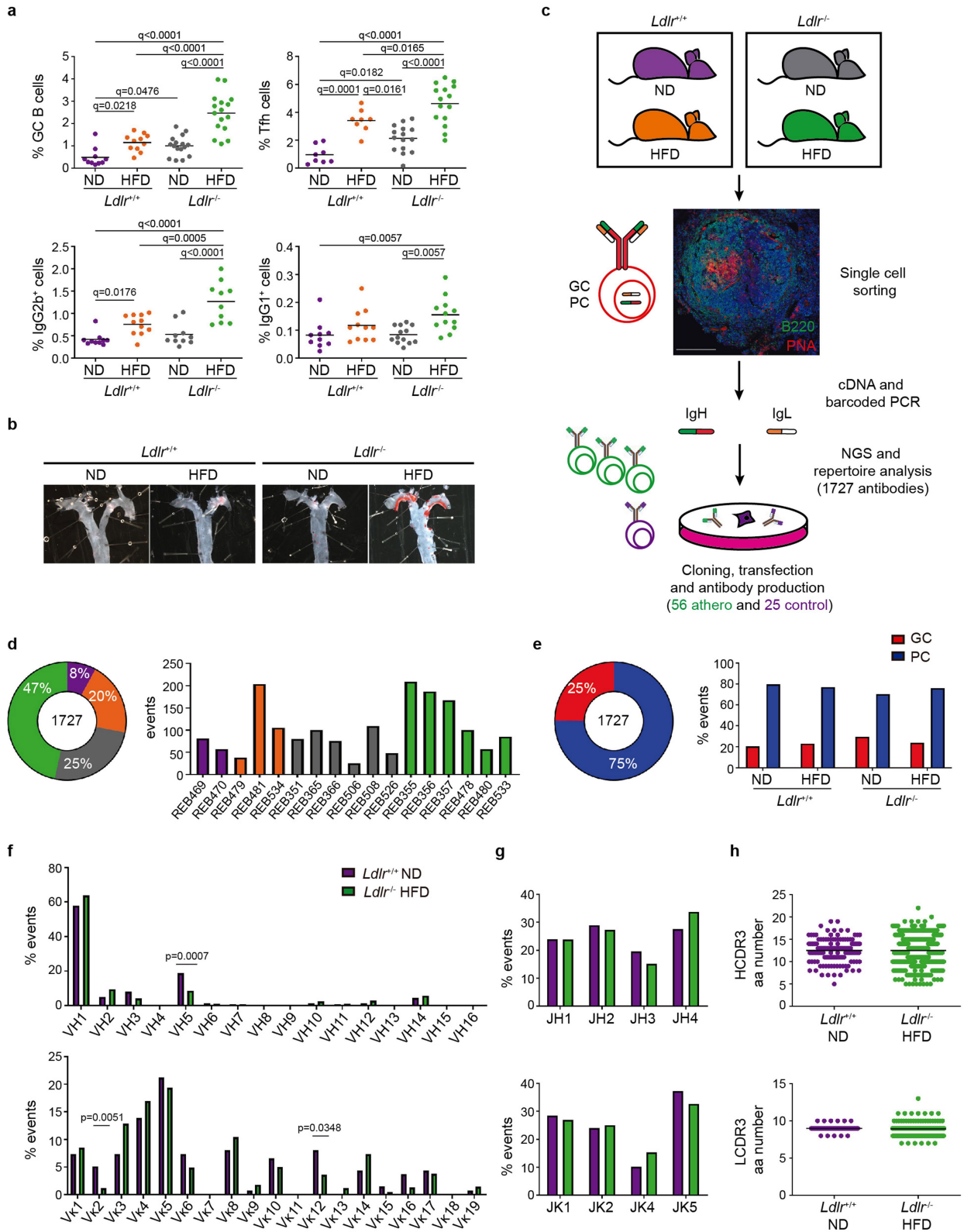
Extended Data Fig. 3 | See next page for caption.

Article

**Extended Data Fig. 3 | Identification of atherosclerosis-associated antibodies by single-cell sequencing and cloning of immunoglobulin genes. a**, Frequency of germinal centre B cells (Fas$^+$GL7$^+$, gated on B220$^+$) ($n = 10$ $Ldlr^{+/+}$ ND, $n = 11$ $Ldlr^{+/+}$ HFD, $n = 16$ $Ldlr^{-/-}$ ND/HFD mice), T follicular helper (Tfh) cells (CXCR5$^+$PD-1$^+$, gated on CD4$^+$) ($n = 8$ $Ldlr^{+/+}$ ND/HFD, $n = 15$ $Ldlr^{-/-}$ ND/HFD mice), and B cells expressing class-switched immunoglobulins (IgG2b ($n = 10$ $Ldlr^{+/+}$ ND, $n = 11$ $Ldlr^{+/+}$ HFD, $n = 10$ $Ldlr^{-/-}$ ND/HFD mice), IgG1 ($n = 10$ $Ldlr^{+/+}$ ND, $n = 11$ $Ldlr^{+/+}$ HFD, $n = 13$ $Ldlr^{-/-}$ ND, $n = 12$ $Ldlr^{-/-}$ HFD mice)) in the spleen of $Ldlr^{+/+}$ and $Ldlr^{-/-}$ mice after 16 weeks of ND/HFD treatment. Statistical analysis was done with one-way ANOVA. **b**, Representative Oil-Red-stained *en face* aortas from $Ldlr^{+/+}$ or $Ldlr^{-/-}$ mice fed with ND or HFD for 16 weeks. **c**, Cell isolation and antibody expression-cloning strategy. Individual spleen germinal centre B cells and plasma cells from $Ldlr^{+/+}$ ND ($n = 2$, purple), $Ldlr^{+/+}$ HFD ($n = 3$, orange), $Ldlr^{-/-}$ ND ($n = 6$, grey), and $Ldlr^{-/-}$ HFD ($n = 6$, green) were isolated by single-cell sorting. IgH and IgL cDNAs from sorted cells were then PCR amplified and sequenced. Successful paired (IgH + IgL) sequences were obtained for a total of 1727 individual cells. 56 antibodies representative of expanded B cell clones (clusters) from atherogenic mice ($Ldlr^{-/-}$ HFD) were cloned into expression vectors containing the human IgG1 constant region for IgH and the kappa constant region for IgL, as described[37]. Expression vectors were transfected in eukaryotic cells, and antibodies were harvested from supernatants for further analysis. As controls, 25 antibodies from $Ldlr^{+/+}$ ND mice were cloned and expressed in eukaryotic cells. **d**, *Left* Distribution of the 1727 events in the four groups of mice. *Right* Number of events per mouse. **e**, *Left* Overall proportion of germinal centre B cells and plasma cells in the sequenced events. *Right* Proportion of germinal centre B cells and plasma cells in each mouse group. **f**–**h**, Data summarize the *Igh* and *Igl* gene sequence analysis from single germinal centre B cells and plasma cells from $Ldlr^{+/+}$ ND mice (138 antibodies) and $Ldlr^{-/-}$ HFD mice (805 antibodies). *Igh* and *Igl* V gene family **(f)** and J gene usage **(g)**. **h**, IgH and IgL CDR3 amino acid number of the antibodies from $Ldlr^{+/+}$ ND ($n = 138$ antibodies) and $Ldlr^{-/-}$ HFD ($n = 805$ antibodies) mice. Statistical analysis was done with two-sided Fisher exact test.
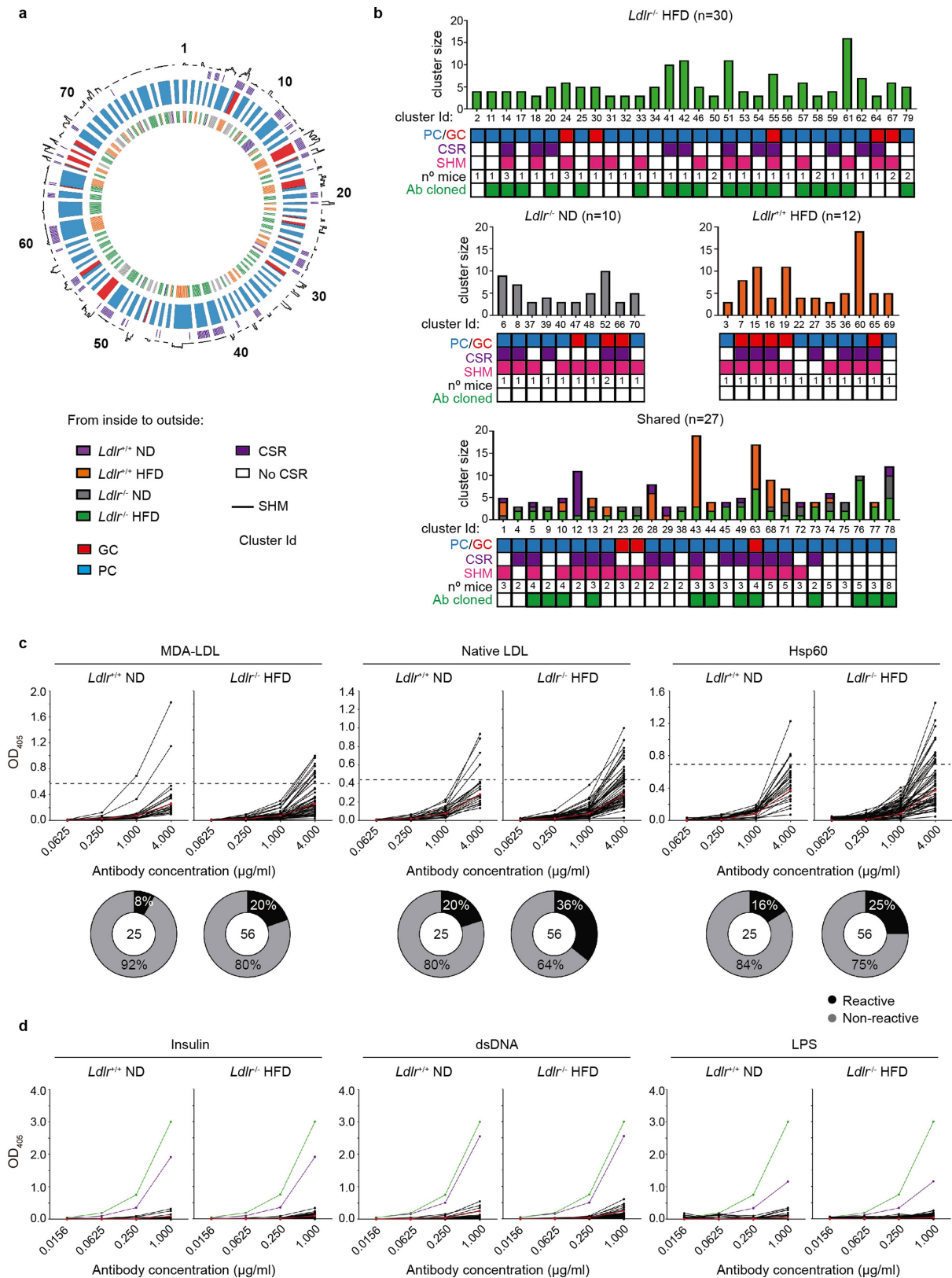
Extended Data Fig. 4 | Analysis of clonally related B cell clusters. a, Circos plot representation of the molecular features of the identified expanded clonally related cells. **b**, Cluster summary. Bars show cluster size (number of antibodies). Checked boxes underneath indicate the population or origin (PC/germinal centre), the presence of CSR and SHM, and the number of mice sharing the cluster. Green-checked boxes indicate the antibodies cloned for subsequent analysis. **c**, Antibodies cloned from control mice (*n* = 25) and atherogenic mice (*n* = 56) were tested by ELISA for their reactivity against MDA-LDL, native LDL, and Hsp60. The charts show OD_{405} values at 4 μg/ml antibody and at three consecutive 1:4 dilutions. Red lines represent the non-reactive negative control antibody mGO53[39]. The proportion of antibodies showing reactivity is shown below each graph. **d**, Antibodies were tested for polyreactivity with insulin, dsDNA, and LPS. As controls, we used the highly polyreactive ED38 antibody (green lines), low-polyreactive JB40 antibody (purple lines), and non-polyreactive mGO53 antibody (red lines)[39].

a

b
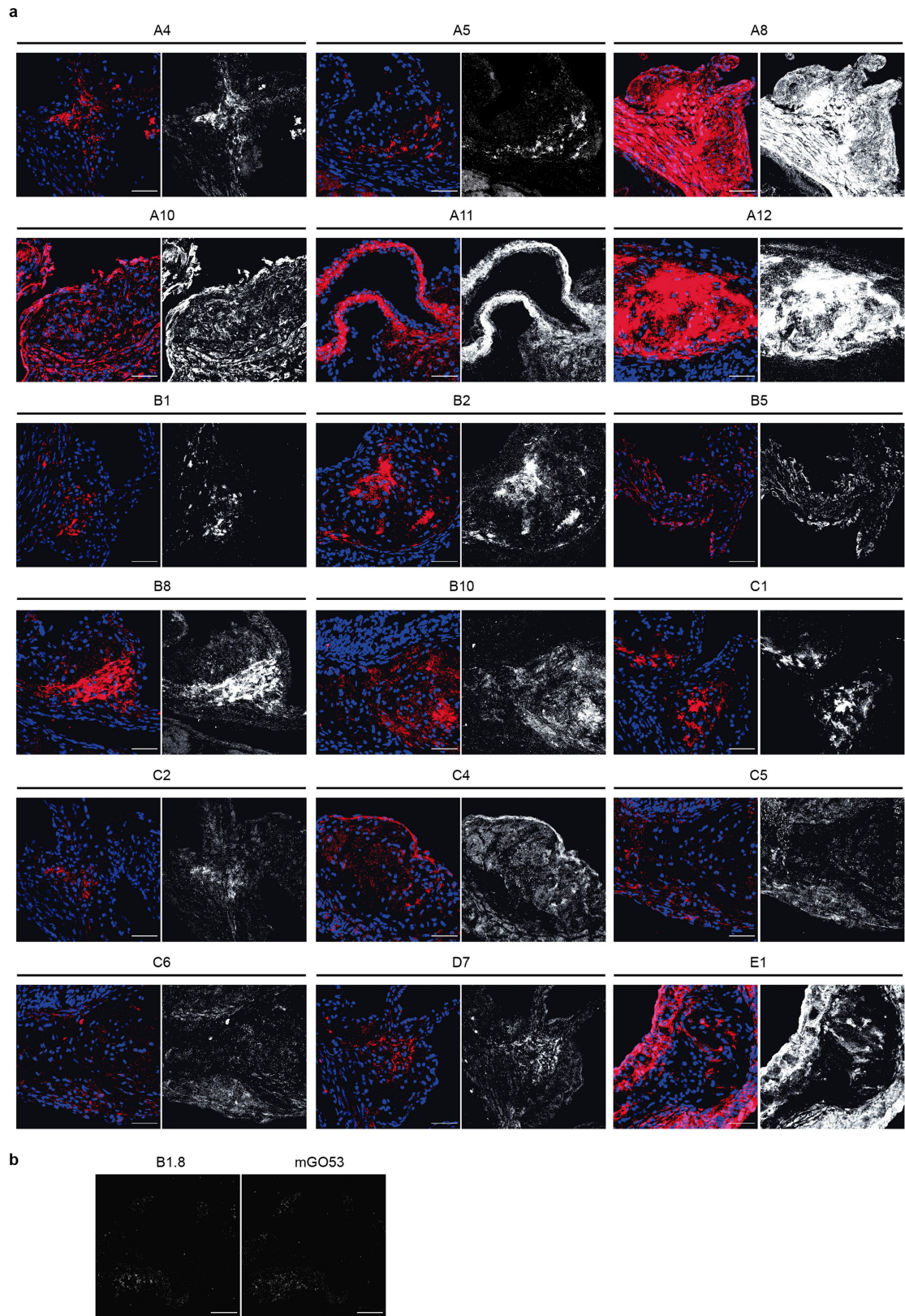
Extended Data Fig. 5 | Plaque reactivity of antibodies cloned from *Ldlr*^{−/−} HFD mice. a, Representative staining of aortic sinus cryosections from *Ldlr*^{−/−} HFD mice with the 18 plaque reactive antibodies from *Ldlr*^{−/−} HFD mice. The left panel of each image pair shows merged antibody staining (red) and Dapi (blue). The right panels show the antibody signal alone (white). 40x magnification; scale bar = 50 µm. **b**, Sections stained with B1.8 and mGO53 control antibodies. 10x magnification; scale bar = 200 µm. **a**, **b**, Maximum intensity Z-projection images are shown.
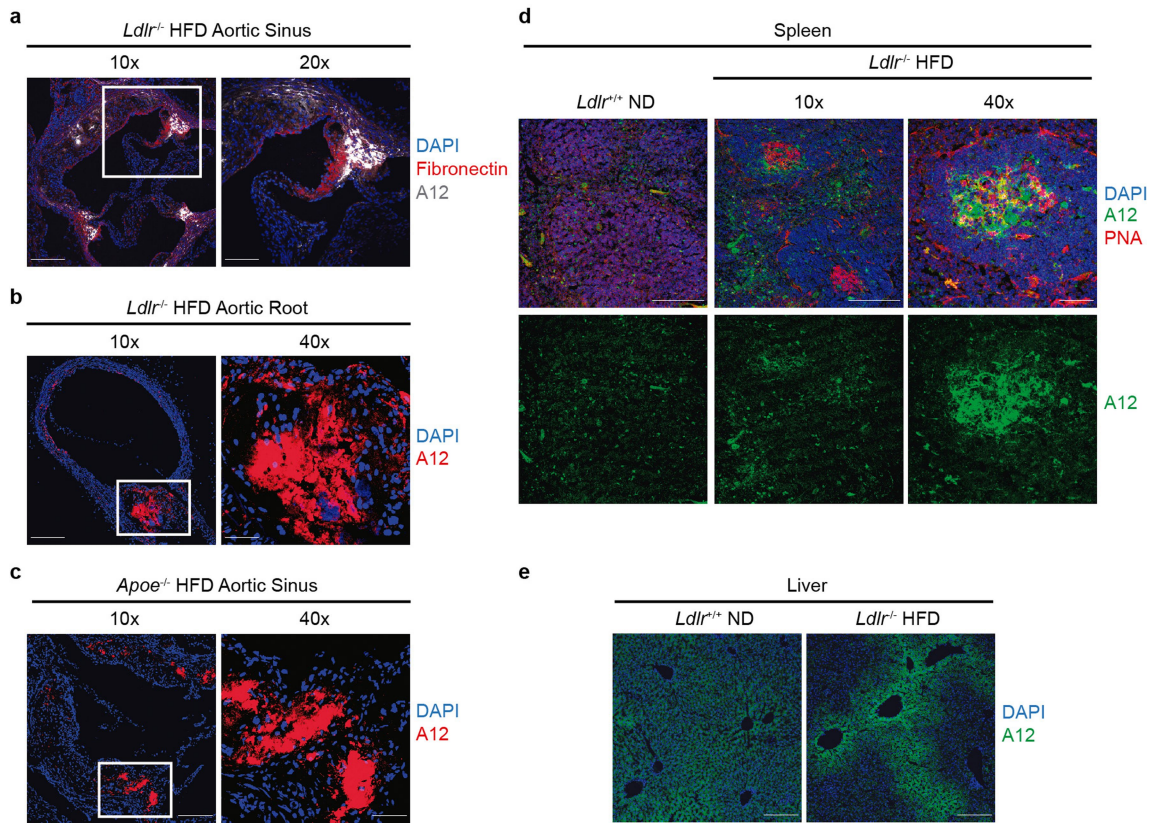
Extended Data Figure 6 | Immunofluorescence analysis of A12 reactivity. a, Representative staining with A12 antibody (white) and fibronectin (red) in aortic sinus cryosections from *Ldlr*^{−/−} HFD mice. **b**, Representative staining with A12 antibody (red) in aortic root cryosections from *Ldlr*^{−/−} HFD mice. **c**, Representative staining with A12 antibody (red) in aortic sinus cryosections from *Apoe*^{−/−} HFD mice. **d**, A12 staining (green) on spleen sections from wild-type and *Ldlr*^{−/−} HFD mice, co-stained with PNA (red). **e**, A12 staining (green) on liver sections from wild-type and *Ldlr*^{−/−} HFD mice. Scale bar 10x= 200 μm; 20x=100 μm; 40x= 50 μm. **a**–**e**, Maximum intensity Z-projection images are shown.

a

Enrichment (IP/input)

IP Antibody: A10 A11 A12 D7 CT E9 CT B1.8

● *Ldlr*+/+ ND
● *Ldlr*-/- HFD

b

OD405

Antibody concentration (µg/ml)

■ anti-ALDH4A1
■ A12
■ mGO53

c

A12 bound to ALDH4A1 (B/B0)

Competitor (µg/ml)

● BSA
● MDA-LDL
● ALDH4A1

d

IgM anti-ALDH4A1

Time (weeks)

● *Ldlr*+/+ ND
● *Ldlr*-/- HFD

q=0.0037

e

IgG anti-ALDH4A1

p=0.0258

Ldlr+/+ ND   *Ldlr*-/- HFD

f

Aortic sinus ALDH4A1

Ldlr+/+ ND | *Ldlr*-/- HFD

5x | 5x | 20x

g

Liver ALDH4A1

Ldlr+/+ ND | *Ldlr*-/- HFD

h

% Abundance

ALDH4A1 | Mitochondrial proteins | ACTB

● Healthy
● Fatty streak   } Media
● Fibrolipid lesion

● Fatty streak   } Intima
● Fibrolipid lesion

i

|	p	O.R. (IC 95%)
Age	0.025	1.146 (1.017-1.291)
Diabetes	0.481	1.602 (0.432-5.937)
Smoking	0.435	1.511 (0.536-4.262)
HTA	0.102	2.598 (0.833-7.676)
CVD	0.218	2.455 (0.588-10.248)
Dyslipidemia	0.030	3.347 (1.127-9.942)
CRP	0.134	1.174 (0.952-1.448)
ALDH4A1 (per 10 units)	0.027	1.275 (1.027-1.583)

Extended Data Fig. 7 | See next page for caption.

**Extended Data Fig. 7 | ALDH4A1 mitochondrial auto-antigen is recognized by A12 antibody and correlates with atherosclerosis in mice and humans.** **a**, Enrichment of ALDH4A1 in each immunoprecipitation (PSM IP/PSM input) ($n = 3$ independent experiments). **b**, ELISA validation of A12 specificity for ALDH4A1. Plates were coated with ALDH4A1-FLAG and incubated either with mGO53 antibody[39] (negative control), A12, or anti-ALDH4A1 (positive control). Data represent the relative absorbance at 405 nm. **c**, Competition immunoassay of A12 antibody (1 μg/ml) binding to plated mouse ALDH4A1-FLAG protein in the presence or absence of increasing amounts (0, 50, 100, 200, 400 μg/ml) of the indicated competitors (BSA, MDA-LDL or ALDH4A1-FLAG). Results are shown as ratios of A12 binding to ALDH4A1-FLAG in the presence (B) or absence (B0) of the competitor. **d**, ELISA determination of anti-ALDH4A1 IgM antibody levels in plasma from $Ldlr^{+/+}$ ND mice (purple, $n = 5$) and $Ldlr^{-/-}$ HFD mice (green, $n = 8$) at the indicated times of ND or HFD feeding. Statistical analysis was done with two-way ANOVA. **e**, ELISA determination of

anti-ALDH4A1 IgG antibody levels in plasma from $Ldlr^{+/+}$ ND mice (purple, $n = 10$) and $Ldlr^{-/-}$ HFD mice (green, $n = 10$) after 16 weeks of diet treatment. Statistical analysis was done with two-tailed unpaired Student's t-test. **f**, Representative immunohistochemistry staining with anti-ALDH4A1 antibody on aortic sinus sections from wild type and $Ldlr^{-/-}$ HFD mice. Scale bars, 5x = 200 μm; 20x = 50 μm. **g**, ALDH4A1 staining in liver sections from wild type and $Ldlr^{-/-}$ HFD mice. Scale bar = 50 μm. **h**, Quantification of the abundance of ALDH4A1 protein, all mitochondrial proteins and ACTB actin in the medial and intimal layers of human samples (healthy ($n = 6$ (ALDH4A1), $n = 9$ (mitochondrial proteins and ACTB)); fatty streak lesion ($n = 4$ (ALDH4A1), $n = 7$ (mitochondrial proteins and ACTB) for media, $n = 6$ for intima)); and fibrolipid lesion ($n = 8$ (ALDH4A1), $n = 11$ (mitochondrial proteins and ACTB) for media, $n = 12$ for intima)). **i**, Logistic regression analysis adjusted with cardiovascular risk factors was performed with atherosclerosis presence as dependent variable.
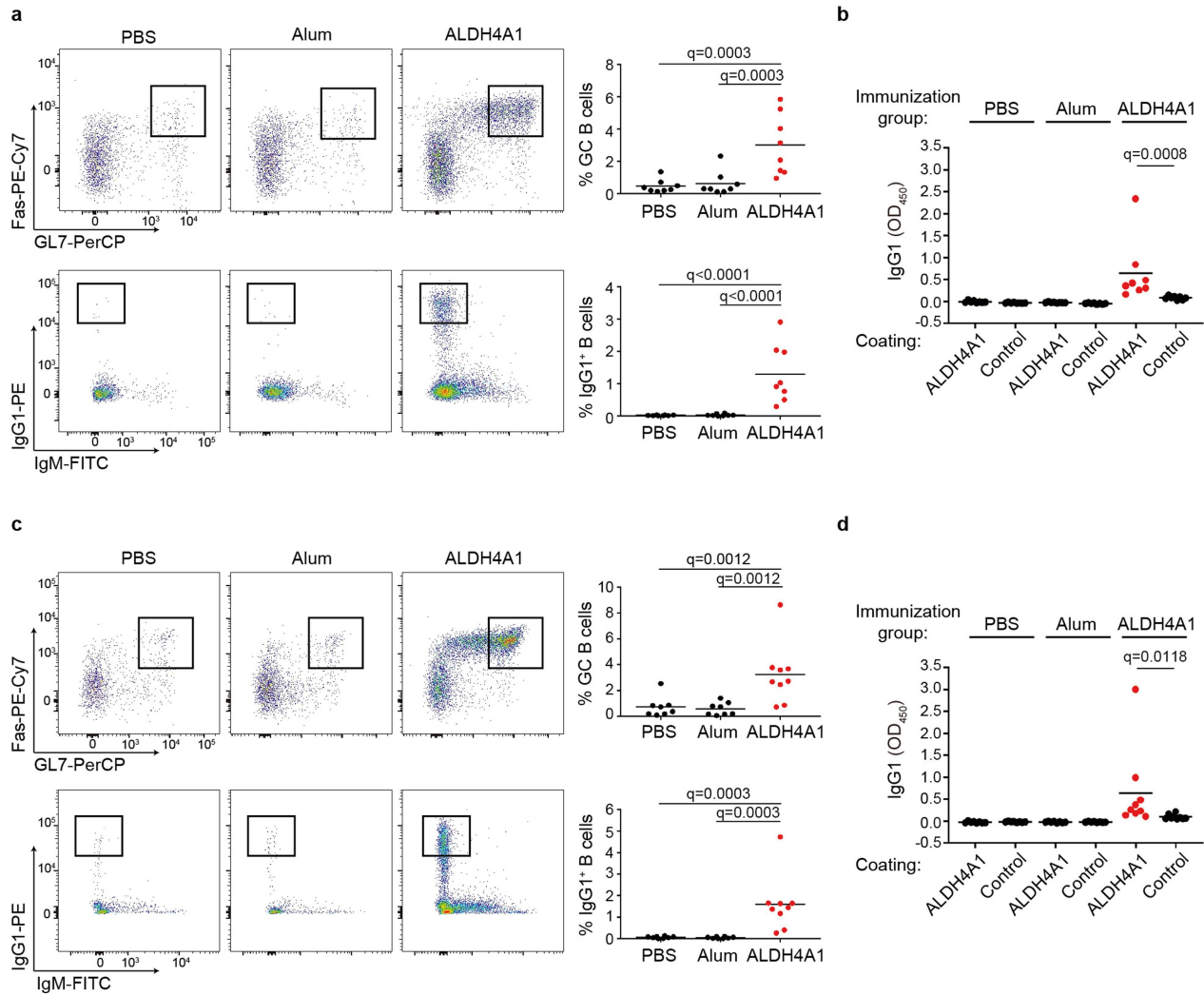
Extended Data Fig. 8 | ALDH4A1 triggers a T-cell dependent B cell response. 6-7-week-old wild type (**a**, **b**) or *Ldlr*^{−/−} (**c**, **d**) mice were immunized with ALDH4A1-FLAG protein plus alum (ALDH4A1 group; a and b, *n* = 8, c and d, *n* = 9). Control mice were injected with alum only (ALUM group; a and b, *n* = 8, c and d, *n* = 8) or with PBS (PBS group; a and b, *n* = 8, c and d, *n* = 8). Mice were sacrificed and the immune response in lymph nodes was analysed by flow cytometry and ELISA. **a**, **c**, Left, representative flow cytometry plots of germinal centre B cells (Fas⁺GL7⁺, gated on B220⁺) and IgG1⁺ B cells (gated on B220⁺). Right, quantification. **b**, **d**, ELISA quantification of IgG1 antibodies specific for ALDH4A1 protein. Plates were coated with ALDH4A1-FLAG protein or IKAROS-FLAG as control protein and incubated with plasma from mice from the indicated immunization groups. Plots represents the relative absorbance at 450 nm. Statistical analysis was done with one-way ANOVA.
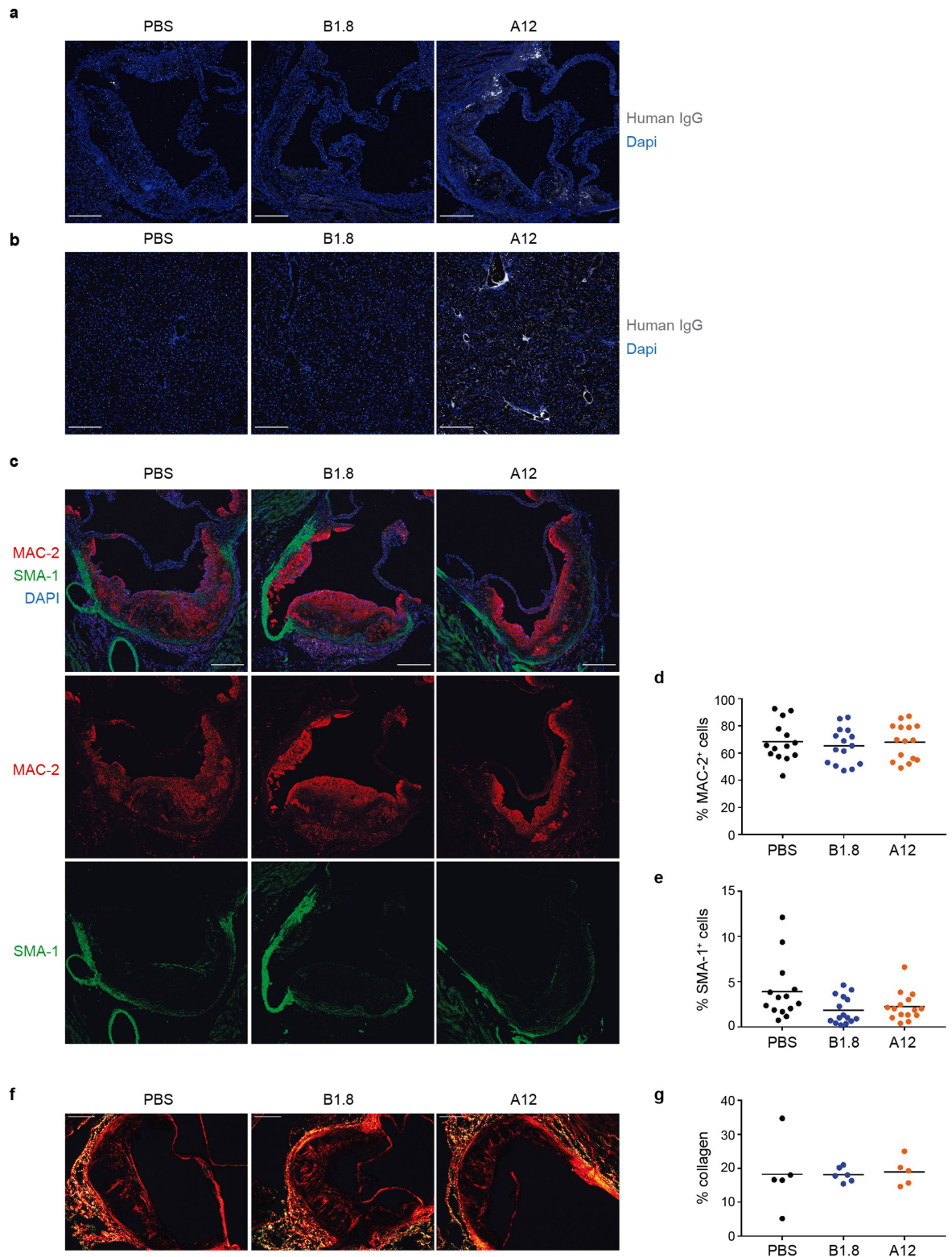
Extended Data Fig. 9 | Evaluation of atheroma plaque and liver composition after A12 antibody treatment. a, **b**, *Ldlr*^{−/−} mice were fed with HFD for 12 weeks, infused with hA12-IgG1 (*n* = 5 mice), hB18-IgG1 (*n* = 4 mice) or PBS (*n* = 4 mice) and sacrificed 3 or 7 days later. Representative staining of aortic sinus **(a)** and liver **(b)** cryosections with anti-human IgG antibody is shown. Scale bar 10x = 200 μm. Maximum intensity Z-projection images are shown. **c**, Representative MAC-2 (red) and SMA-1 (green) immunofluorescence in aortic sinus cryosections from *Ldlr*^{−/−} HFD mice treated with PBS, B1.8, or A12. Scale bar 10x = 200 μm. Maximum intensity Z-projection images are shown. **d**, Plaque macrophage content (% MAC-2^{+}) in *Ldlr*^{−/−} HFD mice treated with PBS (*n* = 14), B1.8 (*n* = 15) or A12 (*n* = 15). **e**, Plaque smooth muscle cell content (% SMA-1^{+}) in *Ldlr*^{−/−} HFD mice treated with PBS (*n* = 14), B1.8 (*n* = 15) or A12 (*n* = 15). **f**, Picrosirius Red staining of aortic sinus cryosections from *Ldlr*^{−/−} HFD mice treated with PBS, B1.8, or A12. Scale bar = 200 μm. **g**, Plaque collagen content in *Ldlr*^{−/−} HFD mice treated with PBS (*n* = 5), B1.8 (*n* = 6) or A12 (*n* = 5).
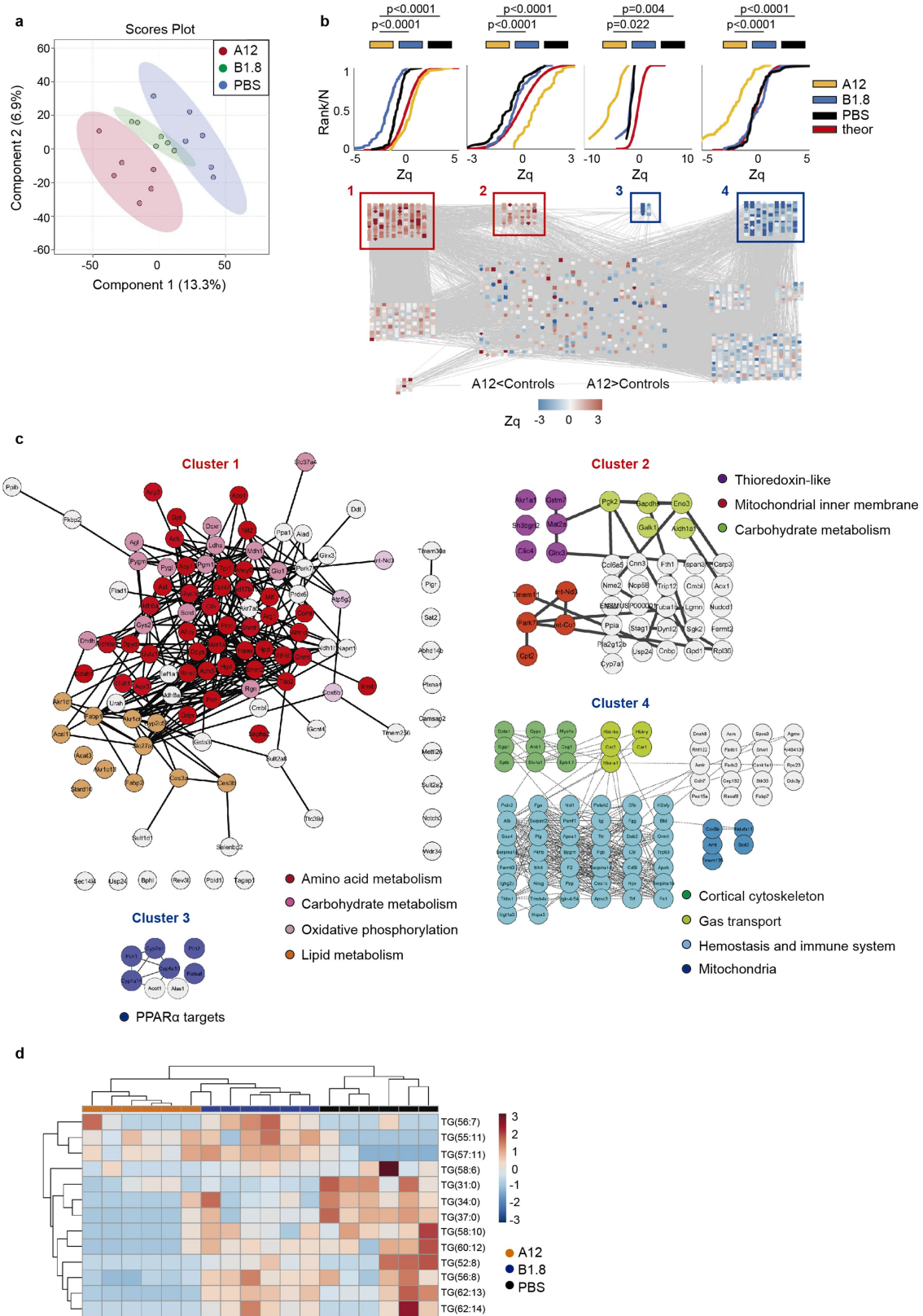
Extended Data Fig. 10 | See next page for caption.

Extended Data Fig. 10 | High-throughput quantitative proteomics of liver from A12-treated mice. Liver from A12-treated mice ($n = 6$) as well as mice treated with PBS ($n = 6$) or with the unrelated control antibody B1.8 ($n = 6$) were subjected to proteomics using multiplexed TMT isobaric labelling. **a**, Principal component analysis (PCA) showed that A12 infusion promotes in the liver a distinct proteome shift, compared to livers from PBS or B1.8 infused mice. **b**, Correlation network analysis using Cytoscape grouped protein abundance changes into four significant clusters (lower panel). Two of them contained proteins that showed a coordinated statistically significant increase (clusters 1 and 2) or decrease (clusters 3 and 4) after A12 treatment in relation to the control treatments (B1.8 or PBS) (upper panels), according to the two-sample Kolmogorov–Smirnov test. **c**, Functional association network and enrichment analysis using STRING revealed that each of these clusters contained groups of functionally-related proteins that were significantly enriched in several biological pathways. The increased proteins in cluster 1 belonged to carbohydrate, amino acid and lipid metabolic pathways, while most of the decreased proteins of cluster 4 belonged to immune system and inflammation pathways. Cluster 3 also contained proteins related to carbohydrate metabolism. Other enriched functional categories are also indicated in the panels. **d**, Clustering result of statistically significant triglycerides (TGs). Heat map was obtained by MetaboAnalyst (distance measure using Euclidean, and clustering algorithm using complete). TGs were putatively identified by searching the m/z against Ceu Mass Mediator (http://ceumass.eps.uspceu.es/mediator/) and considering retention time (RT) prediction and isotopic pattern distribution score in Freestyle (Thermo).

nature research

Corresponding author(s):   Almudena R Ramiro

Last updated by author(s): Sep 22, 2020

Reporting Summary

Nature Research wishes to improve the reproducibility of the work that we publish. This form provides structure for consistency and transparency in reporting. For further information on Nature Research policies, see Authors & Referees and the Editorial Policy Checklist.

Statistics

For all statistical analyses, confirm that the following items are present in the figure legend, table legend, main text, or Methods section.

n/a	Confirmed	
☐	☒	The exact sample size (*n*) for each experimental group/condition, given as a discrete number and unit of measurement
☐	☒	A statement on whether measurements were taken from distinct samples or whether the same sample was measured repeatedly
☐	☒	The statistical test(s) used AND whether they are one- or two-sided *Only common tests should be described solely by name; describe more complex techniques in the Methods section.*
☒	☐	A description of all covariates tested
☐	☒	A description of any assumptions or corrections, such as tests of normality and adjustment for multiple comparisons
☐	☒	A full description of the statistical parameters including central tendency (e.g. means) or other basic estimates (e.g. regression coefficient) AND variation (e.g. standard deviation) or associated estimates of uncertainty (e.g. confidence intervals)
☐	☒	For null hypothesis testing, the test statistic (e.g. *F*, *t*, *r*) with confidence intervals, effect sizes, degrees of freedom and *P* value noted *Give P values as exact values whenever suitable.*
☒	☐	For Bayesian analysis, information on the choice of priors and Markov chain Monte Carlo settings
☒	☐	For hierarchical and complex designs, identification of the appropriate level for tests and full reporting of outcomes
☐	☒	Estimates of effect sizes (e.g. Cohen's *d*, Pearson's *r*), indicating how they were calculated

Our web collection on statistics for biologists contains articles on many of the points above.

Software and code

Policy information about availability of computer code

Data collection	- Flow cytometry data were collected with FACSDiva software v6.1.2. - Single cell sequencing was performed on 454 GS FLX+ and Illumina MiSeq 2x300. - Proteomics and lipidomics data were obtained from mass spectrometers using Xcalibur 2.2 software (Thermo Scientific). - Lipid profile biochemistry was measured with a Dimension RxL Max analyzer (Siemens).
Data analysis	- Flow cytometry data was analyzed with FlowJo v10.4.2 software. - Immunohistochemistry and immunofluorescence images were analyzed with Fiji ImageJ v1.52i. - Statistical analysis were done with GraphPad Prism 7.3 and SPSS (23.0; SPSS, Inc., Chicago) softwares. - Single cell sequencing data processing was done with sciReptor v1.0.2-3-ga48fc90 and v1.1-2-gf4cf8e2. - Sequences and cloning strategy were analyzed with SeqBuilder software (Lasergene 12.2.0). - Protein identification was performed using Proteome Discoverer 2.1 (Thermo Scientific). Protein quantification and statistical analysis was performed using the SanXot 1.0 package. Further analysis were performed using Cytoscape 3.6.1 and String v11. - Lipid quantification was performed using Compound Discoverer 2.1 (Thermo Scientific). Lipidome analysis was performed using CEU Mass Mediator 3.0 and Metaboanalyst 4.0.

For manuscripts utilizing custom algorithms or software that are central to the research but not yet described in published literature, software must be made available to editors/reviewers. We strongly encourage code deposition in a community repository (e.g. GitHub). See the Nature Research guidelines for submitting code & software for further information.

Data

All manuscripts must include a data availability statement. This statement should provide the following information, where applicable:

- Accession codes, unique identifiers, or web links for publicly available datasets
- A list of figures that have associated raw data
- A description of any restrictions on data availability

Antibody sequences are available from ENA under PRJEB34262 Project. Proteomics data are available on Peptide Atlas ftp://PASS01505:VE2555mc@ftp.peptideatlas.org/ and ftp://PASS01607:CP3575gq@ftp.peptideatlas.org/. Lipidomics data are available at the NMDR website, Project ID PR000985.

Field-specific reporting

Please select the one below that is the best fit for your research. If you are not sure, read the appropriate sections before making your selection.

☒ Life sciences   ☐ Behavioural & social sciences   ☐ Ecological, evolutionary & environmental sciences

For a reference copy of the document with all sections, see nature.com/documents/nr-reporting-summary-flat.pdf

Life sciences study design

All studies must disclose on these points even when the disclosure is negative.

Sample size	Sample sizes were chosen to provide confidence in the results and measurements, based on previous studies. Number of mice used in each experiment is indicated in figure legends and/or Methods.
Data exclusions	Animals were excluded from the analysis when signs of sickness unrelated to atherosclerosis were observed. Specifically, we have observed that a proportion of LDLR-/- HFD mice develop dermatitis pathologies. In order to exclude confounding phenotypes unrelated to atherosclerosis those mice have been systematically excluded in all experiments.
Replication	Experiment replicates are detailed in figure legends and/or Methods, as requested. We confirmed that all attempts at replication were successful.
Randomization	Allocation of mice and samples into groups was random. For human samples, plasma from 56 patients subjected to carotid endarterectomy at IIS-Fundacion Jimenez Diaz and Hospital de Galdakao, and from 54 controls with no carotid stenosis were randomly selected (Table S5).
Blinding	Data acquisition in all the experiments was performed blindly.

Behavioural & social sciences study design

All studies must disclose on these points even when the disclosure is negative.

Study description	*Briefly describe the study type including whether data are quantitative, qualitative, or mixed-methods (e.g. qualitative cross-sectional, quantitative experimental, mixed-methods case study).*
Research sample	*State the research sample (e.g. Harvard university undergraduates, villagers in rural India) and provide relevant demographic information (e.g. age, sex) and indicate whether the sample is representative. Provide a rationale for the study sample chosen. For studies involving existing datasets, please describe the dataset and source.*
Sampling strategy	*Describe the sampling procedure (e.g. random, snowball, stratified, convenience). Describe the statistical methods that were used to predetermine sample size OR if no sample-size calculation was performed, describe how sample sizes were chosen and provide a rationale for why these sample sizes are sufficient. For qualitative data, please indicate whether data saturation was considered, and what criteria were used to decide that no further sampling was needed.*
Data collection	*Provide details about the data collection procedure, including the instruments or devices used to record the data (e.g. pen and paper, computer, eye tracker, video or audio equipment) whether anyone was present besides the participant(s) and the researcher, and whether the researcher was blind to experimental condition and/or the study hypothesis during data collection.*
Timing	*Indicate the start and stop dates of data collection. If there is a gap between collection periods, state the dates for each sample cohort.*
Data exclusions	*If no data were excluded from the analyses, state so OR if data were excluded, provide the exact number of exclusions and the rationale behind them, indicating whether exclusion criteria were pre-established.*
Non-participation	*State how many participants dropped out/declined participation and the reason(s) given OR provide response rate OR state that no participants dropped out/declined participation.*

Randomization	*If participants were not allocated into experimental groups, state so OR describe how participants were allocated to groups, and if allocation was not random, describe how covariates were controlled.*

Ecological, evolutionary & environmental sciences study design

All studies must disclose on these points even when the disclosure is negative.

Study description	*Briefly describe the study. For quantitative data include treatment factors and interactions, design structure (e.g. factorial, nested, hierarchical), nature and number of experimental units and replicates.*
Research sample	*Describe the research sample (e.g. a group of tagged Passer domesticus, all Stenocereus thurberi within Organ Pipe Cactus National Monument), and provide a rationale for the sample choice. When relevant, describe the organism taxa, source, sex, age range and any manipulations. State what population the sample is meant to represent when applicable. For studies involving existing datasets, describe the data and its source.*
Sampling strategy	*Note the sampling procedure. Describe the statistical methods that were used to predetermine sample size OR if no sample-size calculation was performed, describe how sample sizes were chosen and provide a rationale for why these sample sizes are sufficient.*
Data collection	*Describe the data collection procedure, including who recorded the data and how.*
Timing and spatial scale	*Indicate the start and stop dates of data collection, noting the frequency and periodicity of sampling and providing a rationale for these choices. If there is a gap between collection periods, state the dates for each sample cohort. Specify the spatial scale from which the data are taken*
Data exclusions	*If no data were excluded from the analyses, state so OR if data were excluded, describe the exclusions and the rationale behind them, indicating whether exclusion criteria were pre-established.*
Reproducibility	*Describe the measures taken to verify the reproducibility of experimental findings. For each experiment, note whether any attempts to repeat the experiment failed OR state that all attempts to repeat the experiment were successful.*
Randomization	*Describe how samples/organisms/participants were allocated into groups. If allocation was not random, describe how covariates were controlled. If this is not relevant to your study, explain why.*
Blinding	*Describe the extent of blinding used during data acquisition and analysis. If blinding was not possible, describe why OR explain why blinding was not relevant to your study.*

Did the study involve field work? ☐ Yes ☐ No

Field work, collection and transport

Field conditions	*Describe the study conditions for field work, providing relevant parameters (e.g. temperature, rainfall).*
Location	*State the location of the sampling or experiment, providing relevant parameters (e.g. latitude and longitude, elevation, water depth).*
Access and import/export	*Describe the efforts you have made to access habitats and to collect and import/export your samples in a responsible manner and in compliance with local, national and international laws, noting any permits that were obtained (give the name of the issuing authority, the date of issue, and any identifying information).*
Disturbance	*Describe any disturbance caused by the study and how it was minimized.*

Reporting for specific materials, systems and methods

We require information from authors about some types of materials, experimental systems and methods used in many studies. Here, indicate whether each material, system or method listed is relevant to your study. If you are not sure if a list item applies to your research, read the appropriate section before selecting a response.

Materials & experimental systems

n/a	Involved in the study
☐	☒ Antibodies
☐	☒ Eukaryotic cell lines
☒	☐ Palaeontology
☐	☒ Animals and other organisms
☐	☒ Human research participants
☒	☐ Clinical data

Methods

n/a	Involved in the study
☒	☐ ChIP-seq
☐	☒ Flow cytometry
☒	☐ MRI-based neuroimaging

Antibodies

Antibodies used	BD Bioscience: B220 (clone RA3-6B2; 562922), Fas (clone Jo2; 557653), GL7 (553666), CD4 (clone RM4-5; 553048), PD-L2 (clone TY25; 560086), CD138 (clone 281-2; 563193), Igkappa (clone 187.1; 559940), IgG1 (clone A85-1; 550083), IgM (clone IL-41; 550676, 553437), CD16/CD32 (clone 2.4G2; 553142). BioLegend: CXCR5 (clone L138D7; 145505), PD-1 (clone 29F-1A12; 135217), IgG2b (clone RMG2b-1; 406708). AbD Serotec: IgG2c (polyclonal; STAR135F). Acris: oxLDL (polyclonal; AP02084SU-N). ThermoFisher Scientific: SMA-1 (clone 1A4; MS-113-B0). Tebu-Bio: MAC-2 (clone M3/38; CL8942AP). Abcam: ALDH4A1 (EPR14288(B); ab181256), Fibronectin (ab2413). Southern Biotech: IgD (clone 11-26; 1120-08). Bethyl: Goat anti-mouse IgM (A90-101A, A90-101P), goat anti-mouse IgG (A90-131A, A90-131P). The manuscript describes in detail the generation of the recombinant monoclonal antibodies (A12...etc) and its validation.
Validation	All the antibodies used in this study were validated for their indicated applications by the manufacturer: B220, Fas, GL7, CD4, PD-L2, CD138, Igkappa, IgG1, IgM (Flow cytometry, Routinely Tested); CD16/CD32 (Flow cytometry, Blocking, Routinely Tested); CXCR5, PD-1, IgG2b (FC-Quality tested); IgG2c (Flow cytometry, Verified); oxLDL (Immunohistochemistry on Cryosections); SMA-1 (Immunofluorescence); MAC-2 (IHC(F)); ALDH4A1 (WB, IHC-P, IP); Fibronectin (ICC/IF); IgD (Flow Cytometry-Quality tested); Goat anti-mouse IgM and IgG (ELISA).

Eukaryotic cell lines

Policy information about cell lines

Cell line source(s)	HEK293T cells (ATCC® CRL-3216™).
Authentication	None of the cell lines used were authenticated.
Mycoplasma contamination	We confirme that cell lines tested negative for mycoplasma contamination.
Commonly misidentified lines (See ICLAC register)	No commonly misidentified cell lines were used in the study.

Palaeontology

Specimen provenance	N/A
Specimen deposition	N/A
Dating methods	N/A

☐ Tick this box to confirm that the raw and calibrated dates are available in the paper or in Supplementary Information.

Animals and other organisms

Policy information about studies involving animals; ARRIVE guidelines recommended for reporting animal research

Laboratory animals	Mus musculus: 6-10 weeks old males LDLR-/- mice (Jackson Laboratories, 002207); 6-10 weeks old males C57BL/6 mice (Envigo, C57BL/6JOlaHsd); 6-10 weeks old males ApoE-/- mice (Charles River, B6.129P2-Apoetm1Unc/J). All animals were housed in specific pathogen-free conditions, under a 12 h dark/light cycle with food and water ad libitum. Ambient temperature: 20-24 °C; humidity: 45-65%.
Wild animals	The study did not involve wild animals.
Field-collected samples	No field-collected samples were used in the study.
Ethics oversight	Animal procedures were approved by the CNIC Ethics Committee and the Madrid regional authorities (PROEX 377/15) and conformed to EU Directive 2010/63/EU and Recommendation 2007/526/EC regarding the protection of animals used for experimental and other scientific purposes, enforced in Spanish law under Real Decreto 1201/2005.

Note that full information on the approval of the study protocol must also be provided in the manuscript.

Human research participants

Policy information about studies involving human research participants

Population characteristics	For the study involving plasma samples, all the clinical characteristics (including CV risk factors) are shown in Table S5 and their potential as confounding factors has been assessed in the multivariate logistic regression analysis (Extended Data Figure 7i). For the study involving tissue samples, no clinical characteristics are obtained.
Recruitment	Plasma was obtained from 56 patients undergoing carotid endarterectomy (carotid stenosis>70%) in IIS-Fundacion Jimenez Diaz and Hospital de Galdakao and from 54 controls showing no stenosis in the carotid artery who were recruited from a screening program for both carotid atherosclerosis and abdominal aortic aneurysm between 65 years-old men. Aortic samples were

obtained from brain-deceased organ donors during organ removal for therapeutic transplantation (kidney or liver transplantation). No self-selection bias or other biases are present that are likely to impact results.

Ethics oversight	The study involving plasma samples was approved by the ethical committee on human research of IIS-Fundacion Jimenez Diaz (PIC 144-2016). The study involving tissue samples was authorized by the French Biomedicine Agency (PFS 09-007, BRIF BB-0033-00029; AoS BBMRI-EU /infrastructure BIOBANQUE ; No. Access : 2, Last : April 15, 2014. [BIORESOURCE]).

Note that full information on the approval of the study protocol must also be provided in the manuscript.

Clinical data

Policy information about clinical studies

All manuscripts should comply with the ICMJE guidelines for publication of clinical research and a completed CONSORT checklist must be included with all submissions.

Clinical trial registration	*Provide the trial registration number from ClinicalTrials.gov or an equivalent agency.*
Study protocol	*Note where the full trial protocol can be accessed OR if not available, explain why.*
Data collection	*Describe the settings and locales of data collection, noting the time periods of recruitment and data collection.*
Outcomes	*Describe how you pre-defined primary and secondary outcome measures and how you assessed these measures.*

ChIP-seq

Data deposition

☐ Confirm that both raw and final processed data have been deposited in a public database such as GEO.

☐ Confirm that you have deposited or provided access to graph files (e.g. BED files) for the called peaks.

Data access links *May remain private before publication.*	*For "Initial submission" or "Revised version" documents, provide reviewer access links. For your "Final submission" document, provide a link to the deposited data.*
Files in database submission	*Provide a list of all files available in the database submission.*
Genome browser session (e.g. UCSC)	*Provide a link to an anonymized genome browser session for "Initial submission" and "Revised version" documents only, to enable peer review. Write "no longer applicable" for "Final submission" documents.*

Methodology

Replicates	*Describe the experimental replicates, specifying number, type and replicate agreement.*
Sequencing depth	*Describe the sequencing depth for each experiment, providing the total number of reads, uniquely mapped reads, length of reads and whether they were paired- or single-end.*
Antibodies	*Describe the antibodies used for the ChIP-seq experiments; as applicable, provide supplier name, catalog number, clone name, and lot number.*
Peak calling parameters	*Specify the command line program and parameters used for read mapping and peak calling, including the ChIP, control and index files used.*
Data quality	*Describe the methods used to ensure data quality in full detail, including how many peaks are at FDR 5% and above 5-fold enrichment.*
Software	*Describe the software used to collect and analyze the ChIP-seq data. For custom code that has been deposited into a community repository, provide accession details.*

Flow Cytometry

Plots

Confirm that:

☒ The axis labels state the marker and fluorochrome used (e.g. CD4-FITC).

☒ The axis scales are clearly visible. Include numbers along axes only for bottom left plot of group (a 'group' is an analysis of identical markers).

☒ All plots are contour plots with outliers or pseudocolor plots.

☒ A numerical value for number of cells or percentage (with statistics) is provided.

Methodology

Sample preparation

Single-cell suspensions were obtained from spleen and stained with fluorophore/biotin-conjugated antibodies to detect mouse antigens.

Instrument

LSRFortessa or FACSCanto instruments (BD Biosciences).

Software

FlowJo V10.4.2.

Cell population abundance

Absolute cell numbers of the populations analysed by FACs are now provided in the Extended Data Figure 1b.

Gating strategy

In all cases, only single alive lymphocytes were analyzed:
- Germinal Center (GC) B cells: Fas+GL7+, gated on B220+.
- T follicular helper (Tfh) cells: CXCR5+PD-1+, gated on CD4+.
- Memory B cells: PD-L2+, gated on B220+.
- Plasma cells (PC): CD138+IgK+, gated on alive cells.
- IgG1, IgG2b or IgG2c B cells: IgG1+ or IgG2b+ or IgG2c+, gated on B220+, IgM-IgD-.
The gating strategy is provided now in Extended Data Figure 1A.

☒ Tick this box to confirm that a figure exemplifying the gating strategy is provided in the Supplementary Information.

Magnetic resonance imaging

Experimental design

Design type

Indicate task or resting state; event-related or block design.

Design specifications

Specify the number of blocks, trials or experimental units per session and/or subject, and specify the length of each trial or block (if trials are blocked) and interval between trials.

Behavioral performance measures

State number and/or type of variables recorded (e.g. correct button press, response time) and what statistics were used to establish that the subjects were performing the task as expected (e.g. mean, range, and/or standard deviation across subjects).

Acquisition

Imaging type(s)

Specify: functional, structural, diffusion, perfusion.

Field strength

Specify in Tesla

Sequence & imaging parameters

Specify the pulse sequence type (gradient echo, spin echo, etc.), imaging type (EPI, spiral, etc.), field of view, matrix size, slice thickness, orientation and TE/TR/flip angle.

Area of acquisition

State whether a whole brain scan was used OR define the area of acquisition, describing how the region was determined.

Diffusion MRI ☐ Used   ☐ Not used

Preprocessing

Preprocessing software

Provide detail on software version and revision number and on specific parameters (model/functions, brain extraction, segmentation, smoothing kernel size, etc.).

Normalization

If data were normalized/standardized, describe the approach(es): specify linear or non-linear and define image types used for transformation OR indicate that data were not normalized and explain rationale for lack of normalization.

Normalization template

Describe the template used for normalization/transformation, specifying subject space or group standardized space (e.g. original Talairach, MNI305, ICBM152) OR indicate that the data were not normalized.

Noise and artifact removal

Describe your procedure(s) for artifact and structured noise removal, specifying motion parameters, tissue signals and physiological signals (heart rate, respiration).

Volume censoring

Define your software and/or method and criteria for volume censoring, and state the extent of such censoring.

Statistical modeling & inference

Model type and settings

Specify type (mass univariate, multivariate, RSA, predictive, etc.) and describe essential details of the model at the first and second levels (e.g. fixed, random or mixed effects; drift or auto-correlation).

Effect(s) tested

Define precise effect in terms of the task or stimulus conditions instead of psychological concepts and indicate whether ANOVA or factorial designs were used.

Specify type of analysis: ☐ Whole brain   ☐ ROI-based   ☐ Both

Statistic type for inference
(See [Eklund et al. 2016](#))

Specify voxel-wise or cluster-wise and report all relevant parameters for cluster-wise methods.

Correction

Describe the type of correction and how it is obtained for multiple comparisons (e.g. FWE, FDR, permutation or Monte Carlo).

Models & analysis

n/a	Involved in the study
☐ ☐	Functional and/or effective connectivity
☐ ☐	Graph analysis
☐ ☐	Multivariate modeling or predictive analysis

Functional and/or effective connectivity

Report the measures of dependence used and the model details (e.g. Pearson correlation, partial correlation, mutual information).

Graph analysis

Report the dependent variable and connectivity measure, specifying weighted graph or binarized graph, subject- or group-level, and the global and/or node summaries used (e.g. clustering coefficient, efficiency, etc.).

Multivariate modeling and predictive analysis

Specify independent variables, features extraction and dimension reduction, model, training and evaluation metrics.